

Nashiro, K.*, Min, J.*, Yoo, H. J.*, Cho, C., Bachman, S., Dutt, S., Thayer, J. F., Lehrer, P., Feng, T., Mercer, N., Nasser, P., Wang, D., Chang, C., Marmarelis, V., Narayanan, S., Nation, D., and Mather, M. (in press). Increasing coordination and responsivity of emotion-related brain regions with a heart rate variability biofeedback randomized trial. (*co-first author) *Cognitive, Affective, & Behavioral Neuroscience*.

Increasing coordination and responsivity of emotion-related brain regions with a heart rate variability biofeedback randomized trial

Kaoru Nashiro¹, Jungwon Min¹, Hyun Joo Yoo¹, Christine Cho¹, Shelby L. Bachman¹, Shubir Dutt¹, Julian F. Thayer², Paul Lehrer³, Tiantian Feng¹, Noah Mercer¹, Padideh Nasser¹, Diana Wang¹, Catie Chang⁴, Vasilis Z. Marmarelis¹, Shri Narayanan¹, Daniel A. Nation², and Mara Mather^{1*}

¹University of Southern California, ²University of California, Irvine, ³Rutgers University, ⁴Vanderbilt University

Corresponding author: Mara Mather, 3715 McClintock Avenue Los Angeles, CA 90089 USA, (213) 821-1868, mara.mather@usc.edu

Abstract

Heart rate variability is a robust biomarker of emotional well-being, consistent with the shared brain networks regulating emotion regulation and heart rate. While high heart rate oscillatory activity clearly indicates healthy regulatory brain systems, can increasing this oscillatory activity also enhance brain function? To test this possibility, we randomly assigned 106 young adult participants to one of two 5-week interventions involving daily biofeedback that either increased heart rate oscillations (Osc+ condition) or had little effect on heart rate oscillations (Osc- condition) and examined effects on brain activity during rest and during regulating emotion. While there were no significant changes in the right amygdala-medial prefrontal cortex (MPFC) functional connectivity (our primary outcome), the Osc+ intervention increased left amygdala-MPFC functional connectivity and functional connectivity in emotion-related resting-state networks during rest. It also increased down-regulation of activity in somatosensory brain regions during an emotion regulation task. The Osc- intervention did not have these effects. In this healthy cohort, the two conditions did not differentially affect anxiety, depression or mood. These findings indicate that modulating heart rate oscillatory activity changes emotion network coordination in the brain.

Introduction

Pacemaker cells within the heart automatically drive heart beats (Monfredi et al., 2010). However, signals from the brain and body, such as those stimulated by breathing and blood pressure oscillations, introduce variability into this otherwise relatively steady rhythm. The dominant source of these oscillatory signals to the heart is the parasympathetic vagus nerve (Reyes del Paso et al., 2013). Hundreds of previous studies have identified vagal heart rate variability (HRV) at rest as one of the best indicators of well-being (Beauchaine & Thayer, 2015; Geisler et al., 2010; Kemp & Quintana, 2013). Vagal HRV refers to HRV measures that reflect relatively high frequency (HF) heart rate oscillations (HF-HRV) or changes in the length of adjacent intervals between heart beats (root mean square of successive differences; RMSSD). These relatively faster changes in heart rate are transmitted by the vagus nerve rather than via sympathetic nerves (Reyes del Paso et al., 2013). At rest, these vagal HRV measures are highly correlated with respiratory sinus arrhythmia, or the degree to which heart rhythms synchronize with breathing. When inhaling, heart rate typically speeds up, and when exhaling, heart rate typically slows down, due to signals transmitted between the brain and the heart via the vagus nerve. Thus, the variability associated with better emotional well-being is not just random noise but instead reflects heart rate oscillations synchronized with breathing.

Why should having a heart rate that responds more to breathing be associated with better emotional well-being? One potential explanation is that many of the brain regions involved in coordinating heart rhythms, such as the ventromedial prefrontal cortex, anterior cingulate cortex, insula and amygdala, are also involved in regulating emotions (Thayer et al., 2012; Thayer & Lane, 2009). Indeed, individual differences in vagal HRV have been linked with brain structures and circuits associated with emotion regulation (Koenig et al., 2021; Sakaki et al., 2016; Thayer

et al., 2012; Yoo et al., 2018). However, heart rate oscillations may go beyond signaling the functioning of regulatory brain regions. They may increase coordination within emotion-related brain networks, improving the brain's capacity to regulate emotion (Mather & Thayer, 2018). Indeed, recent findings from biofeedback studies in which people increase their own heart rate oscillatory activity suggest that episodes of high amplitude heart rate oscillations reduce stress and anxiety (Goessl et al., 2017). In the typical heart rate oscillation biofeedback intervention, people slowly breathe at around 10s/breath or 0.1 Hz while receiving feedback on how much their current heart rate is oscillating in response to their breathing during daily training sessions for a few weeks (Lehrer et al., 2013). Breathing at this pace creates especially high amplitude heart rate oscillations because 0.1 Hz is a resonance frequency for the baroreflex system, which also produces oscillations in heart rate (Lehrer & Gevirtz, 2014).

Intriguingly, ~ 0.1 Hz oscillations in heart rate and breathing are also seen during some meditative practices (Lehrer et al., 1999; Peng et al., 2004; Peng et al., 1999), including during reciting either a yoga mantra or the rosary Ave Maria (Bernardi et al., 2001). Varied cultural practices may have converged on this resonance breathing frequency that creates high oscillations in heart rate because of its positive impact on well-being.

Why would daily time spent in a high physiological oscillatory state increase resting-state coordination within emotion-related brain networks? First consider what occurs during the experience of emotions or feelings. At each moment, the brain receives diverse input about current body states, with the vagus nerve serving as a primary conduit of visceral information (Hagemann et al., 2003; Poppa & Bechara, 2018; Smith et al., 2017). Mapping these body states in the brain is necessary to generate feelings even when the body state is not currently present (Damasio & Carvalho, 2013). That is, people can simulate body state changes in insula and

somatosensory cortices, influencing current feeling states (Bechara & Damasio, 2005; Keysers et al., 2010). This system allows for top-down modulation over feelings and emotions, as prefrontal, anterior cingulate and anterior insula regions both respond to and modulate activity in brain regions mapping visceral and somatic sensations.

Cortical brain regions involved in autonomic control including the insula and ventromedial prefrontal cortex respond to increasing or decreasing heart period intervals, supporting feedback loops that control blood flow to different areas of the body, modulate heart rate, and provide rapid responses to arterial blood pressure changes. Inducing large heart rate oscillations may potentiate these feedback loops, strengthening the ability of autonomic control processes to respond to changes in somatosensory inputs, which in turn should enhance the ability to modulate fluctuations in one's own feelings. If inducing heart rate oscillations strengthens dynamic control over emotion regulation in this way, the effects should be evident during times when the system is challenged by stimuli that induce emotions. These same feedback loops likely contribute to resting-state activity in emotion-related brain regions. Thus, daily sessions spent in a high physiological oscillatory state may also increase the coordinated activity of emotion-related resting-state brain networks (Mather & Thayer, 2018).

Our study (ClinicalTrials.gov NCT03458910; Heart Rate Variability and Emotion Regulation or "HRV-ER") examined whether daily biofeedback sessions stimulating heart rate oscillatory activity in baroreflex frequencies affect the function of brain networks involved in emotion regulation, even when people are not engaged in the biofeedback. We randomly assigned 106 healthy young adults to receive either 'increase-oscillations' (Osc+) or 'decrease-oscillations' (Osc-) biofeedback in daily training sessions for five weeks in a 7-week study involving pre- and post-intervention assessments (see Supplementary Fig. 1 for study schedule

and Fig. 1 and Supplementary Tables 1-2 for participant information). Participants came into the lab weekly as part of small groups and the two groups received similar rationales for their training protocols (Fig. 2A-B).

Figure 1

Flow diagram of the number of participants who enrolled, were allocated to condition, and completed pre- and post-intervention measures; the number of participants or responses available for analysis for each measure are also provided (see text for details regarding exclusion criteria).

Enrollment

Randomized (n=121)

Allocation

Allocated to intervention (n=63)
◆ Completed allocated **Osc+** intervention (n=56)
◆ Did not receive allocated intervention (dropped out) (n=7)

Allocated to intervention (n=58)
◆ Completed allocated **Osc-** intervention (n=50)
◆ Did not receive allocated intervention (dropped out) (n=8)

Pre-Intervention Measures

MRI completed (n=55)
Non-MRI measures completed
◆ Questionnaire
◆ Depression (CES-D) (n_{responses}=112)
◆ Emotional Intensity Rating (n=52)

MRI completed (n=48)
Non-MRI measures completed
◆ Questionnaire
◆ Depression (CES-D) (n_{responses}=100)
◆ Emotional Intensity Rating (n=46)

Throughout Study

Non-MRI measures completed
◆ Heart rate oscillations during training and seated rest (n_{sessions}=2785)
◆ Questionnaires
◆ Mood (POMS) (n_{responses}=391)
◆ Anxiety (SAI) (n_{responses}=390)

Non-MRI measures completed
◆ Heart rate oscillations during training and seated rest (n_{sessions}=2659)
◆ Questionnaires
◆ Mood (POMS) (n_{responses}=344)
◆ Anxiety (SAI) (n_{responses}=343)

Post-Intervention Measures

MRI completed (n=52)
Non-MRI measures completed
◆ Questionnaire
◆ Depression (CES-D) (n_{responses}=112)
◆ Emotional Intensity Rating (n=52)

MRI completed (n=48)
Non-MRI measures completed
◆ Questionnaire
◆ Depression (CES-D) (n_{responses}=98)
◆ Emotional Intensity Rating (n=46)

Analysis

- ◆ Practice completion (n=56)
- ◆ Heart rate oscillations during training and seated rest (n=52)
- ◆ Change in breathing rate during resting-state scan (n=43)
- ◆ Change in breathing rate during emotion regulation scan (n=45)
- ◆ Breathing rate during training-mimicking scan (n=42)
- ◆ Change in etCO₂ during resting state-scan (n=25)
- ◆ Change in etCO₂ during emotion regulation scan (n=24)
- ◆ etCO₂ during training-mimicking scan (n=38)
- ◆ Heart rate variability spectral frequency analyses of resting-state scan (n=36)
- ◆ Resting state functional connectivity (n=49)
- ◆ Arterial spin labeling (n=33)
- ◆ Emotion Regulation Scan (n=45)
- ◆ Emotional Intensity Rating (n=44)
- ◆ Questionnaires
 - ◆ Depression (CES-D) (n_{responses}=223)
 - ◆ Mood (POMS) (n_{responses}=387)
 - ◆ Anxiety (SAI) (n_{responses}=386)
- ◆ Other Measures of Heart Rate Activity (n_{sessions}=333)
- ◆ Post-Study Participant Perceptions of Interventions (n=55)

- ◆ Practice completion (n=50)
- ◆ Heart rate oscillations during training and seated rest (n=45)
- ◆ Change in breathing rate during resting-state scan (n=41)
- ◆ Change in breathing rate during emotion regulation scan (n=34)
- ◆ Breathing rate during training-mimicking scan (n=38)
- ◆ Change in etCO₂ during resting state-scan (n=21)
- ◆ Change in etCO₂ during emotion regulation scan (n=21)
- ◆ etCO₂ during training-mimicking scan (n=35)
- ◆ Heart rate variability spectral frequency analyses of resting-state scan (n=37)
- ◆ Resting state functional connectivity (n=47)
- ◆ Arterial spin labeling (n=33)
- ◆ Emotion Regulation Scan (n=39)
- ◆ Emotional Intensity Rating (n=39)
- ◆ Questionnaires
 - ◆ Depression (CES-D) (n_{responses}=197)
 - ◆ Mood (POMS) (n_{responses}=344)
 - ◆ Anxiety (SAI) (n_{responses}=342)
- ◆ Other Measures of Heart Rate Activity (n_{sessions}=268)
- ◆ Post-Study Participant Perceptions of Interventions (n=49)

A challenge for investigating how HRV biofeedback affects brain functioning is that the blood oxygen level dependent (BOLD) signal is sensitive to changes in breathing rate and carbon dioxide (CO₂) levels. Thus, the main targets of our investigation were the effects of the biofeedback that carried over to the rest of the day, during normal breathing. We tested our hypotheses that the Osc+ intervention would affect both the connectivity of emotion networks during rest and these networks' responsiveness to acute challenges by comparing post-pre resting-state connectivity in emotion-related networks as well as brain activity during an emotion regulation task.

When preregistering our outcomes, we focused on amygdala-related effects of the intervention, due to our prior findings of relationships between amygdala functional connectivity and HRV (Sakaki et al., 2016) and findings that the amygdala is the primary target of emotion regulation control processes (Buhle et al., 2014). Our main outcome measure was pre-to-post intervention changes in resting-state right amygdala functional connectivity with a medial prefrontal cortex (mPFC) region associated with HRV (Thayer et al., 2012). We predicted that relative to the Osc- intervention, the Osc+ intervention would show a greater increase in resting-state functional connectivity between the right amygdala and the mPFC. In the current report, we also included functional connectivity between the left amygdala and the mPFC as an outcome measure, given prior findings indicating the relevance of the left amygdala to HRV (Thayer et al., 2012). As secondary emotion-related outcomes, we examined changes in up- and down-regulation of amygdala activity and self-reported emotion regulation effectiveness during viewing emotional pictures, as well as changes in ratings of emotional well-being. We hypothesized that relative to the Osc- intervention, the Osc+ intervention would show greater amygdala activity during up-regulation and reduced amygdala activity during down-regulation.

In addition, we predicted that Osc+ participants would show greater improvements in self-reported emotion regulation effectiveness and emotional well-being than Osc- participants. In the current report, in addition to the amygdala-focused fMRI outcomes, we also reported our exploratory analyses on the broader context of how the biofeedback affected canonical resting-state networks during rest and brain activity throughout the brain during emotion regulation. Secondary outcome measures also included HRV during rest and measures of cerebral blood flow. Other secondary outcome measures (e.g., decision making, stress responsivity and cognition) will be reported elsewhere. The analyses involving heart rate oscillations are presented as a manipulation check (i.e., this outcome was not explicitly preregistered).

Methods

Participants

We recruited 121 participants aged between 18 and 35 years via the USC Healthy Minds community subject pool, a USC online bulletin board, Facebook and flyers (see Fig. 1 for more details and drop-out rates per condition; see the supplementary methods section for power considerations). Participants provided informed consent approved by the University of Southern California (USC) Institutional Review Board. Prospective participants were screened and excluded for major medical, neurological, or psychiatric illnesses. We excluded people who had a disorder that would impede performing the HRV biofeedback procedures (e.g., coronary artery disease, angina, cardiac pacemaker), who currently were training using a relaxation, biofeedback or breathing practice, or were on any psychoactive drugs other than antidepressants or anti-anxiety medications. We included people who were taking antidepressant or anti-anxiety medication and/or attending psychotherapy only if the treatment had been ongoing and

unchanged for at least three months and no changes were anticipated. Gender, education, age and race were similar in the two conditions (Supplementary Tables 1 and 2).

Overview of 7-week Protocol Schedule

Participants visited the lab weekly for 7 weeks. In the first lab visit we collected non-MRI baseline measures, including questionnaires assessing mood and anxiety (Supplementary Fig. 1). In the second lab visit, we collected the baseline MRI scans and then conducted the participant's first biofeedback training session. We asked participants to engage in daily biofeedback practice between the second and seventh lab visits (approximately five weeks). Participants were instructed to practice 20 minutes/day for the first week of training, 30 minutes/day for the second week of training and 40 minutes/day for the remaining weeks. During the Week 3-6 lab visits, participants shared their experiences and tips about biofeedback training with other participants from the same condition in small groups, while 1-2 researchers facilitated the discussion. Outside the lab, participants used a customized social app to communicate with other members of their group and researchers about their progress on daily biofeedback training. The sixth lab visit repeated the assessments from the first lab visit. The seventh lab visit repeated the baseline MRI session followed by additional training-session scans. After the scan, participants completed a post-study questionnaire.

Biofeedback Training

Osc+ Condition. Participants wore an ear sensor to measure their pulse. The sensor cable was connected to a USB module plugged into a USB port on the training laptop computer. They viewed real-time heart rate biofeedback on the laptop screen via the emWave pro software (Heartmath, 2016) while breathing in through the nose and out through the mouth in synchrony with a visual pacer on the right side of the biofeedback display. During the second lab visit,

participants tried out several breathing paces around 10s/breath or 0.1 Hz to see which induced the largest oscillations in their heart rate (i.e., their own resonance frequency; Lehrer et al., 2013). More specifically, participants were asked to breathe at five different paces for 5 minutes each (9s, 10s, 11s, 12s, and 13s per breath, which approximately corresponds with 6.5, 6, 5.5, 5, and 4.5 breaths per minute as in Lehrer et al. (2013)). To identify each participant's best approximate resonance frequency, we calculated various aspects of the oscillatory dynamics for each breathing pace episode using Kubios HRV Premium 3.1 software and assessed which one had the most of the following characteristics: highest LF power, the highest maximum LF amplitude peak on the spectral graph, highest peak-to-trough amplitude, cleanest and highest-amplitude LF peak and highest RMSSD. Additionally, we included coherence scores associated with each breathing pace episode as one of the characteristics we evaluated (see below for details on the coherence score).

To complete home training, participants received an ear sensor and a small laptop with the emWave Pro software. During their home training, participants breathed to a pacer set to their resonance frequency determined in their prior lab visit. They received biofeedback on their heart rate oscillatory activity via a real-time plot of their heart rate and a 'coherence' score, which is a built-in metric score provided by the emWave Pro software. The software also provided feedback with a green, blue or red light, indicating high, medium or low coherence score, respectively. Coherence is characterized by a sine-wave-like pattern in the HRV waveform in the low frequency (LF) range (McCraty et al., 2009). Thus, a higher coherence score is reflected in the HRV power spectrum as a large increase in power in the LF band around 0.1 Hz. Participants were instructed to aim for a high coherence score. The '**coherence**' score was calculated as $\text{peak power}/(\text{total power} - \text{peak power})$. Peak power was determined by finding the

highest peak within the range of 0.04 – 0.26 Hz and calculating the integral of the window 0.015 Hz above and below this highest peak. Total power was computed for the 0.0033 – 0.4 Hz range.

In the third visit, participants returned to the lab to receive coaching from researchers who checked again which breathing frequency produced the largest heart rate oscillations (i.e., which was likely to approximate resonance frequency). Participants were asked to breathe at three different paces for 5 minutes each: the best approximated resonance frequency from the second week's visit, a one second per breath shorter and a one second per breath longer than their second week's best pace (e.g., if 10s was their second week's best pace, they tried 9s, 10s and 11s per breath). As in the second week, we evaluated the aforementioned characteristics of these three paces and assigned the participant the pace that best approximated their resonance frequency for home training that week.

In the fourth visit, participants were asked to breathe at two different paces for 5 minutes each: the best approximated resonance frequency from the third week's visit and another that was one second per breath longer than their third week's best pace. Participants were also asked to try out abdominal breathing with pursed lips (Lehrer et al., 2013) and other strategies of their choice (e.g., occasionally closing eyes) to help increase their coherence score. Their best approximated resonance frequency was determined in the same way as previously described. During their remaining home training, participants were asked to breathe at the resonance frequency determined in their fourth lab visit and use strategies that they found most effective (e.g., abdominal breathing).

Osc- Condition. An ideal comparison to this Osc+ intervention would be another condition with similar biofeedback information, participant expectations, and time spent training, but no increases in heart rate oscillatory activity during the training sessions. However, most

relaxing states increase heart rate oscillations (Terathongkum & Pickler, 2004). To address this, we designed a decrease-oscillations comparison condition (Osc-) in which participants received heart rate biofeedback aimed at reducing their heart rate oscillations during the training sessions. In addition, to avoid having them discover that they could reduce HRV simply by increasing physical activity (Sarmiento et al., 2013), we asked them to also try to reduce their heart rate during the training sessions.

In the second lab visit, participants were asked to come up with five strategies to reduce heart rate and heart rate oscillations (e.g., imagining the ocean, listening to nature sounds, listening to instrumental music). Participants used the same biofeedback ear sensor device and emWave Pro software as Osc+ participants to view real-time heart rate biofeedback while they tried each strategy for five minutes. We analyzed the data in Kubios and identified which strategy had the most of the following characteristics: lowest LF power, the minimum LF amplitude peak on the spectral graph, lowest peak to trough amplitude, multiple and lowest-amplitude LF peak and lowest RMSSD. In addition, we included calmness scores (see below for details) as one of the characteristics we evaluated.

To complete home training, participants received an ear sensor and a small laptop with a custom software. During their home training, participants aimed to reduce heart rate and heart rate oscillations using the best strategy determined in their prior lab visit. The custom-developed software provided a '**calmness**' score (an 'anti-coherence' score), which was calculated by multiplying the coherence score that would have been displayed in the Osc+ condition by -1 and adding 10. The net result was that participants got more positive feedback (higher calmness scores) when their heart rate oscillatory activity in the 0.04 – 0.26 Hz range was low (see Supplementary Materials for more details).

In the third visit, participants were asked to select three strategies and try them out for 5 minutes each. The strategy identified as best (based on the same characteristics used at the second lab visit) was selected as the one to focus on during their home training the following week.

In the fourth visit, participants selected two strategies and tried them out for 5 minutes each. The strategy identified as best was selected as the one to focus on during their remaining home training. Example segments of heart rate during rest and during home training are shown for one participant from each condition (Fig. 2C-D).

MRI Scan Session Order

In both the pre- and post-intervention MRI sessions, scans were conducted in the following order: 1) rest during blood oxygen level dependent (BOLD) fMRI; 2) rest during pseudo-continuous arterial spin labeling (pCASL); 3) emotion regulation task during fMRI; and 4) structural scan. The post-intervention session included additional training-mimicking scans (a BOLD fMRI scan followed by a pCASL scan) conducted after these four initial scans so as not to influence them. During these two additional training-mimicking post-intervention scans, participants engaged in their now-daily training practice (see below for details).

MRI Scan Parameters

We employed a 3T Siemens MAGNETOM Trio scanner with a 32-channel head array coil at the USC Dana and David Dornsife Neuroimaging Center. T1-weighted 3D structural MRI brain scans were acquired pre and post intervention using a magnetization prepared rapid acquisition gradient echo (MPRAGE) sequence with TR = 2300 ms, TE = 2.26 ms, slice thickness = 1.0 mm, flip angle = 9°, field of view = 256 mm, and voxel size = 1.0 x 1.0 x 1.0 mm, with 175 volumes collected (4:44 min). Functional MRI scans during the emotion-

regulation task and resting-state scans were acquired using multi-echo-planar imaging sequence with TR= 2400 mm, TE 18/35/53 ms, slice thickness = 3.0 mm, flip angle = 75°, field of view = 240 mm, voxel size = 3.0 x 3.0 x 3.0 mm. We acquired 250 volumes (10 min) for the emotion-regulation task and 175 volumes (7 min) for the resting-state scans. PCASL scans were acquired with TR = 3880, TE = 36.48, slice thickness = 3.0 mm, flip angle = 120°, field of view = 240 mm and voxel size = 2.5 X 2.5 X 3.0 mm, with 12 volumes collected (3:14 min; 1st volume was an M0 image, 2nd volume was a dummy image, and the remaining 10 volumes were 5 tag-control pairs) both during resting-state (pre and post) and training-mimicking (post) scans. This ASL approach provides high precision and signal-to-noise properties and has better test-retest reliability than pulsed or continuous ASL techniques (Chen et al., 2011).

Pre- and Post-Intervention BOLD Resting-state Scan

Participants were instructed to rest, breathe as usual and look at the central white cross on the black screen.

Pre- and Post-Intervention pCASL Resting-state Scan

To assess whether the intervention affected blood flow during rest, in both MRI sessions participants completed a second short resting-state scan. Participants were instructed to rest while breathing normally with their eyes open. To make visual inputs similar to those viewed during the training scan (for our analyses comparing rest vs. training scans), we presented red and blue circles alternately at a random rate (see *Training-Mimicking Sessions During BOLD and PCASL* section below). Participants were asked not to pay attention to these stimuli.

Emotion Regulation Task

Participants completed an emotion regulation task (Kim & Hamann, 2007) in the MRI scanner, which lasted for about 10 min. Each trial consisted of three parts: instruction (1s),

regulation (6s), and rating (4s). First, participants were given one of three instructions: “view”, “intensify,” or “diminish.” Then, during the regulation phase, they saw a positive, neutral or negative image. Finally, they were asked to rate the strength of the feeling they were experiencing on a scale ranging from 1 (very weak) to 4 (very strong).

Before the task, we instructed participants that the cue “intensify” would indicate they should escalate the emotion evoked by the subsequent image to feel the emotion more intensely. On the other hand, we instructed them that the cue “diminish” would indicate they should moderate the emotion elicited by the image in such a way that they felt calmer. We instructed them that the cue “view” meant they should simply look at the image without trying to change the emotion (see Supplementary Materials for more details).

Training-Mimicking Sessions During BOLD and PCASL

In the post-intervention scan session after the resting-state and emotion-regulation scans, participants completed their daily training without biofeedback during BOLD and pCASL scans. By this point, participants were well-trained, having each completed on average 57 training sessions at home. For the Osc+ group, a red and blue circle alternated at their resonance frequency. For example, if their resonance frequency was 12 sec, the red circle was presented for 6 sec followed by the blue circle for 6 sec. Participants were asked to breathe in with the red circle and breathe out with the blue circle. For the Osc- group, the stimuli were the same as the Osc+ group; however, the red and blue circles alternated at a random rate and participants were told not to pay attention to them.

Analyses

Heart Rate Oscillations During Training and Seated Rest. The pulse data recorded by emWave pro software and sensor unit were saved in a database file on the laptop. The database file was also transferred to a remote server via internet connection by custom software. Interbeat interval (IBI) data were exported from the database file for HRV analysis. We used Kubios HRV Premium 3.1 (Tarvainen et al., 2014) to compute autoregressive spectral power for each training session and for the baseline rest session (a 5-min session before lab training session) in the lab in Week 2 (Fig. 2E-F; see Supplementary Materials for more details).

Heart Rate Oscillations and Breathing Rate During fMRI Scans. Both photoplethysmogram (PPG) and breathing data were collected using Biopac MP150 Data Acquisition System using MR-compatible sensors during resting-state and emotion regulation fMRI scans in Weeks 2 and 7. The breathing belt, TSD201 transducer, converted changes in chest circumference to electric voltage signal, which were then 0.05-1Hz bandpass-filtered, amplified with 10 times of gain, sampled at 10kHz using RSP100C. During analyses using MATLAB, the respiration signal was downsampled at 1kHz and smoothed, and two iterations of peak detection were performed to obtain an average breathing rate across each scan duration. The PPG data were collected using a Nonin Medical 8600FO Pulse Oximeter at 10kHz sampling rate and downsampled at 1kHz using MATLAB. PPG data were also analyzed using Kubios HRV Premium Version 3.1 to obtain the frequency value with peak power within the high frequency range (0.15-0.4 Hz).

Preprocessing of fMRI Data. To minimize the effects of motion and non-BOLD physiological effects, we employed multi-echo sequences during our fMRI scans. BOLD T2* signal is linearly dependent on echo time, whereas non-BOLD signal is not echo-time dependent (Kundu et al., 2012). Thus, multi-echo acquisitions allow uncoupling of BOLD signal from

movement artifact and significantly improve accuracy of functional connectivity analyses (Dipasquale et al., 2017), with between 2-3 times the level of reliability of typical single-echo scans (Lynch et al., 2020). We implemented a denoising pipeline using independent components analysis (ICA) and echo-time dependence to distinguish BOLD fluctuations from non-BOLD artifacts including motion and physiology (Kundu et al., 2013).

Resting State Functional Connectivity. Seed-based functional connectivity analysis: The mPFC was defined based on a previous meta-analysis of brain regions where activity correlated with HRV (a sphere of 10mm around the peak voxel, $x=2$, $y=46$, $z=6$; Thayer et al., 2012). The right and left amygdala were each anatomically defined using that participant's T1 image. The segmentation of the right and left amygdala was performed using the FreeSurfer software package version 6 using the longitudinal processing scheme implemented to incorporate the subject-wise correlation of longitudinal data into the processing stream (<http://surfer.nmr.mgh.harvard.edu>; Fischl et al., 2004). Labels from the specific structures (left/right amygdala) were saved as two distinct binary masks in the native space. All files were visually inspected for segmentation accuracy at each time point. We used FSL FLIRT to linearly align each participant's preprocessed data to their brain-extracted structural image and the standard MNI 2-mm brain. We applied a low-pass temporal filter 0-0.1 Hz and extracted time series from the mPFC. For each participant, a multiple regression analysis was performed in FSL FEAT with nine regressors including the mPFC time series, signal from white matter, signal from cerebrospinal and six motion parameters. The individual amygdalae were registered to the standard MNI 2-mm brain using FSL FLIRT using trilinear interpolation followed by a threshold of 0.5 and binarize operation with `fslmaths` to keep the mask a similar size. From each participant's mPFC connectivity map, we extracted the mean beta values from the right and left

amygdalae region-of-interests (ROIs) separately, which represents the strength of functional connectivity with mPFC. Lastly, we performed 2 (condition: Osc+, Osc-) \times 2 (time point: pre, post) mixed ANOVAs on functional connectivity between mPFC and the left amygdala and between mPFC and the right amygdala. P-values were adjusted for multiple comparisons with the Benjamini-Hochberg correction.

Dual regression analysis: The six motion parameters and signal from white matter and cerebrospinal fluid were removed from each participant's preprocessed data. We used FSL FLIRT to linearly align the denoised data to each participant's brain-extracted structural image and the standard MNI 2-mm brain. A low-pass temporal filter 0-0.1 Hz removed high frequency fluctuations. These data were used in a FSL dual-regression analysis (Nickerson et al., 2017), in which we created subject-specific time series based on spatial maps for each of 18 canonical resting state networks from a prior study that linked canonical networks to their functions (Laird et al., 2011). These individual time series were used to create subject-specific spatial maps of each network. From the subject-specific z-transformed spatial maps, we extracted mean functional connectivity values for each participant within an ROI of each of the corresponding canonical network using Laird et al's (Laird et al., 2011) network masks thresholded at 3.1 ($p < 0.001$). We calculated average values within each network category (emotion/interoception, motor/visuospatial, visual, and cognitive) and computed the difference between post and pre functional connectivity values. We were particularly interested in the effects of interventions on five emotion/interoception networks (i.e., Networks 1-5). Network 1 includes primary olfactory and limbic association cortices, involving interoceptive processing and discrimination of emotional pictures and faces. Network 2 encompasses the subgenual anterior cingulate cortex (ACC) and orbitofrontal cortex (OFC), and is associated with olfaction, gustation, and emotion.

Network 3 includes bilateral basal ganglia and thalamus, and is linked to a variety of mental processes, including reward processing, interoceptive functions, pain and somatosensory processing. Network 4 includes bilateral anterior insula/frontal opercula and the anterior aspect of the body of the cingulate gyrus, and is involved in executive function, complex language, affective and interoceptive processes. Network 5 consists of midbrain, and is associated with acupuncture and air-hunger tasks as well as interoceptive stimulation. As comparisons, we included non-emotion networks (i.e., motor/visuospatial, visual and cognition networks) in our analyses. The descriptions of these networks and their associated functions can be found in Laird et al. (2011). We conducted a 2 (condition: Osc+, Osc-) X 2 (network category: emotion/interoception, other.) ANOVA. We then performed post hoc comparisons between conditions for each network category with multiple comparisons with the Benjamini-Hochberg correction.

Arterial Spin Labeling. Data were preprocessed using the Arterial Spin Labeling Perfusion MRI Signal Processing Toolbox (ASLTbx; Wang et al., 2008). M0 calibration image and 10 tag-control pairs were motion corrected, co-registered to individual participants' T1-weighted structural images, smoothed with a 6 mm full width at half maximum Gaussian kernel, and normalized to MNI template space. Preprocessing resulted in a time-series of 5 perfusion images representing the tag-control pairs, which were averaged to create a single mean whole brain perfusion image.

We conducted voxel-wise analyses of whole brain perfusion maps in SPM12 to investigate the effects of training group and time-point on cerebral blood flow with a two-way ANOVA model. We included a study-specific gray matter mask comprised of averaged gray matter segmentations across participants' T1-weighted structural scans in all voxel-wise analyses

to restrict analyses to gray matter cerebral blood flow, as ASL has lower power to detect white matter than gray matter perfusion signal (van Osch et al., 2009). An absolute threshold of 0.01 ml/100g/min was applied to remove background voxels and voxels with negative values.

Following model estimation, we examined interactions of group and scan type (rest pre vs. post; rest pre vs. training), and within-group pre vs. post comparisons.

Emotion Regulation Data. Denoised data were analyzed using FMRIB Software Library (FSL) version 6.0.3 (Jenkinson et al., 2012). Three levels of analyses were performed: individual BOLD signal modeling, post-pre difference within each subject, and testing the difference between groups. For each individual's pre- and post-intervention scans, a standard general linear model estimated BOLD signal during the six seconds of emotion regulation during each trial (see Fig. 4A) with seven regressors: diminish-negative, diminish-positive, intensify-negative, intensify-positive, view-negative, view-positive, and view-neutral. Instruction and rating phases were not modeled. Intensify > view and view > diminish contrasts were conducted across trials combining positive and negative images. We also examined whether the two contrasts differed between positive and negative emotions. This first-level analysis included spatial smoothing with 5-mm FWHM, motion correction (MCFLIRT; Jenkinson et al., 2012), and high-pass filtering with 600s cutoff. Using a 12-degree of freedom linear affine transformation, each participant's BOLD image was registered to a T1-weighted structural image (we registered each pre- vs. post-intervention BOLD image to the T1 image obtained in the same scan session), which was then registered to the MNI-152 T1 2mm brain image. In the second-level analysis, we used FSL's fixed effect model to estimate the post-pre difference within subjects while controlling for the mean effect. In the third-level analysis, we performed mixed-effect analyses to compare the post-pre differences in emotion regulation conditions between the two intervention groups using

FSL's *Randomise* tool with 5,000 permutations and Threshold-Free Cluster Enhancement (TFCE) multiple comparison correction ($p < .05$; Smith & Nichols, 2009).

To test whether the intervention changed amygdala activity during emotion regulation, we extracted amygdala BOLD activity from the results of the second-level analysis using FSL's *featquery* function with binary masks of the left and right amygdala (segmented through the same method used for the resting-state scan analysis and remapped to the standard MNI 2-mm brain). We conducted a univariate ANOVA with the extracted BOLD activity as the dependent variable and condition as a fixed-factor for the Intensify > View and View > Diminish contrasts, separately for the left and right amygdala with the Benjamini-Hochberg correction.

We performed 2 (condition: Osc+, Osc-) \times 2 (time point: pre, post) mixed ANOVAs to test how emotion intensity ratings changed before and after intervention and how the change differed between conditions for each trial type (Diminish, View, and Intensify; 12 trials/trial type) with the Benjamini-Hochberg correction.

Results

The Osc+ intervention increased heart rate oscillations during training but was otherwise well matched with the Osc- intervention.

Participants in the Osc+ vs. Osc- conditions ($N_{Osc+} = 56$; $N_{Osc-} = 50$) did not significantly differ in the average percent of weekly assigned session time they completed ($M = 78.32\%$, $SE = 3.43$ and $M = 82.74\%$, $SE = 3.74$, respectively), $t(104) = -0.87$, $p = .39$, $r = .09$, in the average total amount each participant earned from lab visit payments and group and individual rewards for training adherence and quality ($M = \$293.50$, $SE = \$4.69$ and $M = \$293.42$, $SE = \$5.99$, respectively), $t(104) = 0.01$, $p = .99$, $r = .001$, in the portion of their payment rewards due to

small group performance ($M = \$13.13$, $SE = \$2.11$ and $M = \$15.34$, $SE = \$1.91$, respectively; see Methods for details), $t(104) = -0.77$, $p = .44$, $r = .08$, nor in their post-intervention self-rated difficulty of training, effort, expectations, or plans to continue the intervention techniques (Supplementary Fig. 2). There were no significant effects of condition on the number of people previously diagnosed with major illnesses, $t(104) = -1.65$, $p = .10$, $r = .16$, and the number of people on medication at the time of their study participation, $t(104) = -0.77$, $p = .44$, $r = .08$ (see Supplementary Table 3). There was also no significant effect of condition on heart rate during home training sessions, $F(1,95) = .74$, $p = .39$, $r = .09$. However, as intended, the Osc+ participants increased their heart rate total spectral frequency power during training, $t(51) = 10.15$, $p < .001$, $r = .55$; Fig. 2E), whereas the Osc- participants did not significantly influence this metric compared to their own baseline rest (log transformed autoregressive power difference, $t(44) = 1.49$, $p = .14$, $r = .11$; Fig. 2F), leading to a significant interaction of session type (baseline vs. training) and condition, $F(1,95) = 37.54$, $p < .001$, $r = .53$. In the resonance breathing frequency range (8-16s; .063 Hz~0.125 Hz), the two conditions showed large differences in power during training, $F(1,95) = 44.33$, $p < .001$, $r = .57$.

Figure 2

Comparisons of heart rate oscillatory activity during pre-intervention rest vs. training sessions in the two conditions

HRV training rationale given to participants

A **Osc+**

"Meditation is known to have remarkable effects on emotional health outcomes – it can calm you down and reduces stress and anxiety.

Some meditative practices lead to large but smooth oscillations in the heart, called coherence."

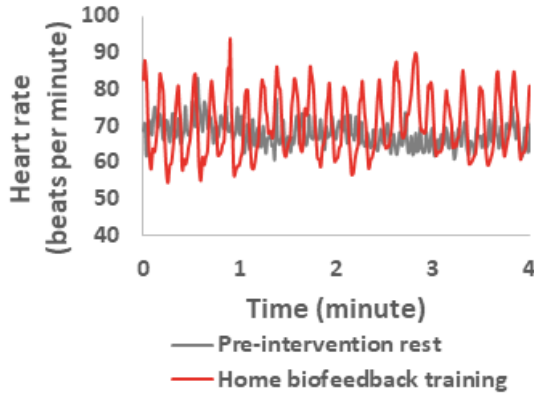
B **Osc-**

"Meditation is known to have remarkable effects on emotional health outcomes – it can calm you down and reduces stress and anxiety.

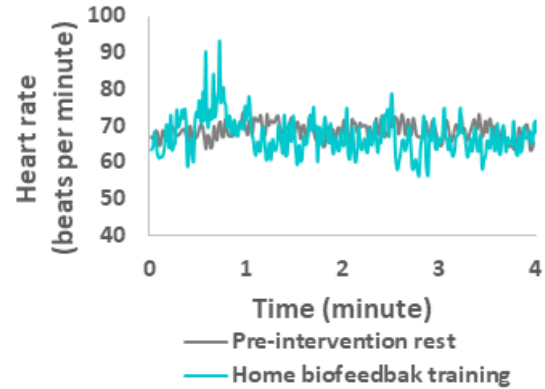
Some meditative practices lead to a low and steady heart rate."

Example 4-min segment from pre-intervention rest vs. home biofeedback training

C

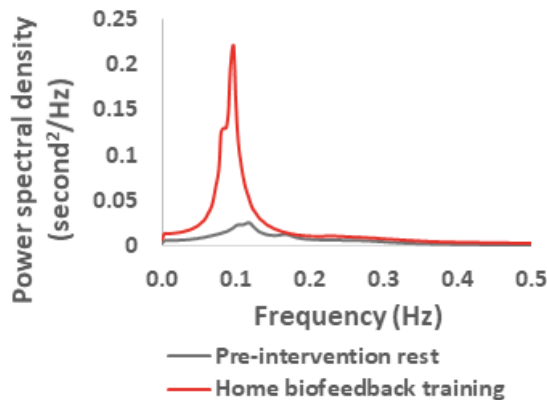


D

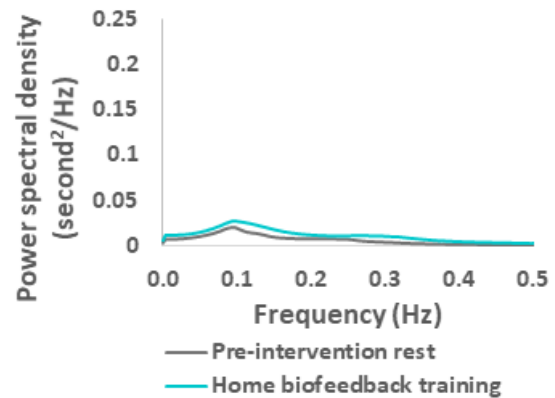


AR spectral power during pre-intervention rest vs. home biofeedback training

E



F



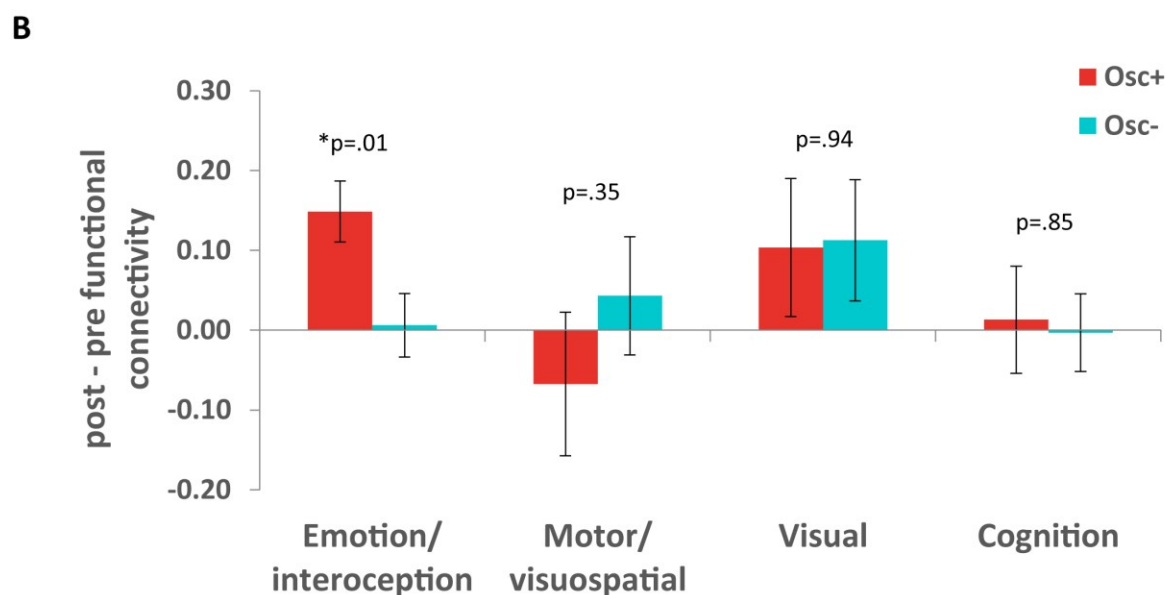
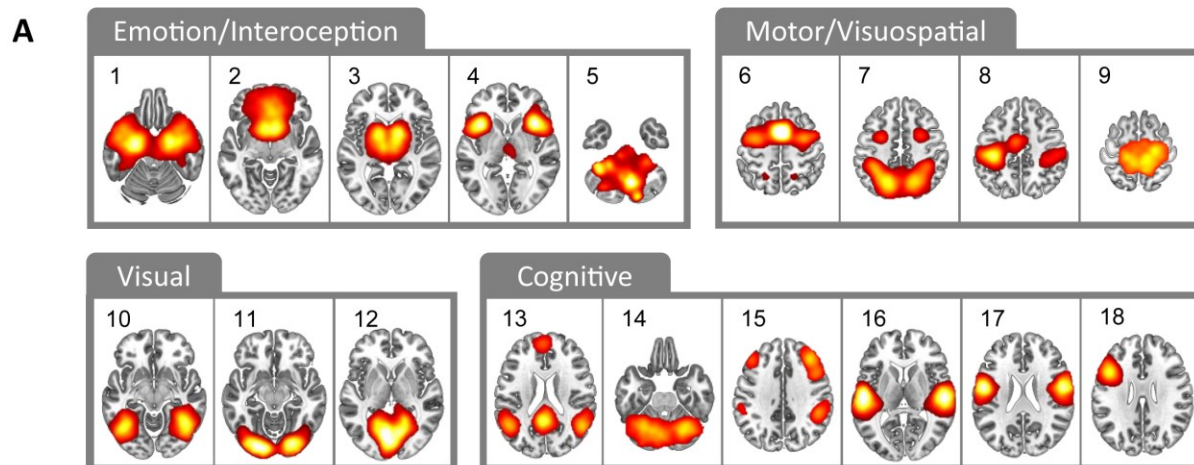
Notes. A-B: Participants received similar motivating background explanations for both conditions; C-D: Example heart rate over time during pre-intervention rest vs. home biofeedback training for an Osc+ (C) vs. an Osc- participant (D); E-F: Autoregressive (AR) spectrum shows large within-condition differences between heart rate oscillatory power during pre-intervention rest vs. home biofeedback training, for Osc+ condition (E) but not Osc- (F) condition. Note that training data in e-f reflect an average across many sessions in participants' homes (training

session N = 5437), whereas pre-intervention resting-state heart rate was measured in one session per participant in the lab.

The Osc+ intervention increased functional connectivity in emotion-related resting-state networks.

Quantification of functional connectivity within 18 canonical resting-state networks revealed that the two HRV biofeedback conditions also affected functional connectivity within emotion-related networks during rest. A 2 (condition: Osc+, Osc-) X 2 (network category: emotion/interoception, other; Fig. 3A) ANOVA yielded a significant interaction of condition and network category, $F(1, 94) = 5.24, p = .024, r = .23$. The Osc+ intervention increased functional connectivity within emotion-related networks significantly more than the Osc- intervention (Fig. 3B), whereas there were no significant differences between conditions for other categories of canonical resting-state networks (for breakdown of intervention effects across all 18 networks separately, see Supplementary Fig. 3).

Figure 3



Notes. We examined changes in canonical resting-state networks (A) from pre- to post-intervention resting scans; Functional connectivity within emotion-related resting state networks also increased significantly more in the Osc+ than the Osc- condition (B). *False Discovery Rate (FDR) $p < .05$. Error bars indicate standard error.

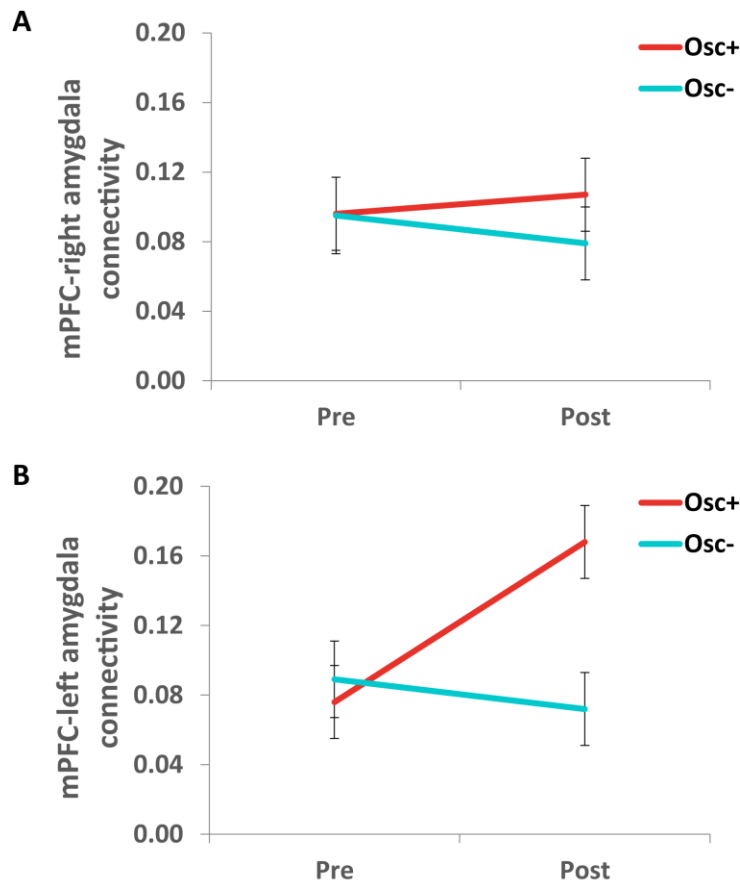
Our primary outcome measure was right amygdala-medial prefrontal cortex (mPFC) functional connectivity, as this is a key emotion-related circuit (Banks et al., 2007; Lee et al., 2012) in which functional connectivity relates to individual differences in heart rate variability

(Sakaki et al., 2016). Seed-based analyses revealed no significant condition by time-point interaction for connectivity between mPFC and the right amygdala, $F(1, 94) = 0.68, p = .41, r = .08$ (Fig. 4A). However, there was a significant interaction of condition by time-point for connectivity between mPFC and the left amygdala, $F(1, 94) = 5.44, p = .02, r = .24$ (Fig. 4B), which was driven by increased connectivity in the Osc+ condition at post intervention, $t(48) = -2.33, p = .02, r = .26$.

Signal from the nearby basal vein of Rosenthal often contaminates BOLD fMRI amygdala signal (Boubela et al., 2015). However, we used multi-echo imaging techniques to remove non-BOLD components such as signal from draining veins (Kundu et al., 2017) and examination of our baseline whole-brain amygdala functional connectivity results indicated that our amygdala signal did not reflect signals from nearby veins (see Supplementary Figure 4).

Figure 4

Functional connectivity between mPFC and amygdala during rest



Notes. MPFC-right amygdala functional connectivity did not differ significantly by condition (A) but mPFC-left amygdala connectivity increased during the intervention in Osc+ participants more than in Osc- participants (B).

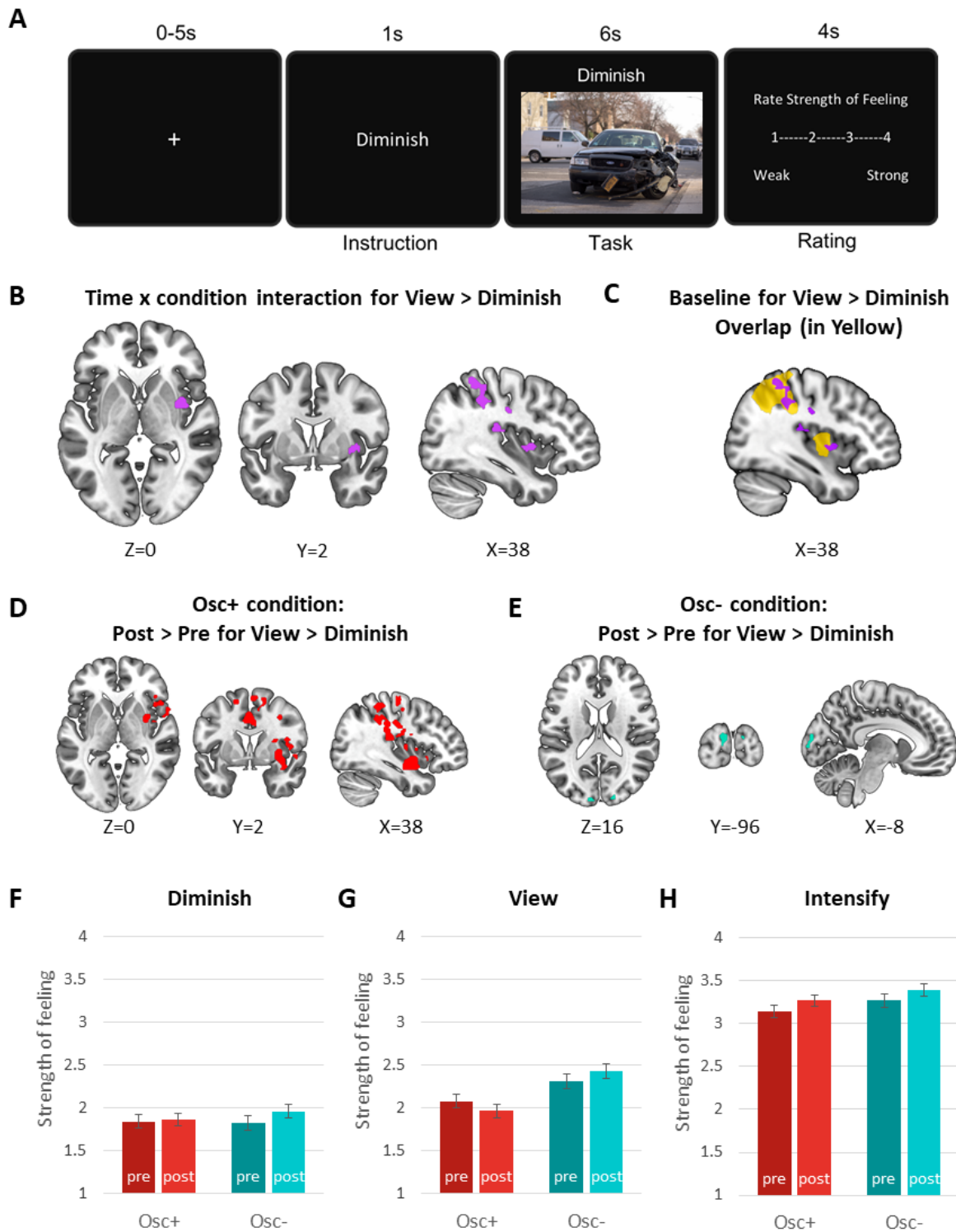
Thus, to summarize so far, the Osc+ intervention affected functional connectivity in emotion-related brain networks, as well as functional connectivity between the left amygdala and mPFC.

The Osc+ intervention increased down-regulation of activity in somatosensory brain regions during an emotion regulation task.

Our next question was how the intervention affected the ability to regulate brain activity associated with emotional experience during externally induced emotional arousal. To test this, both before and after the intervention, participants completed an emotion regulation task during a functional scan of their brain (Fig. 5A). They were allowed to regulate emotions using strategies of their choice, but on post-task questionnaires over 95% of participants indicated relying on cognitive reappraisal strategies.

Figure 5

Trial design and results of the emotion regulation task



Notes. After one of the three instructions (i.e., intensify, diminish or view) was given, participants viewed each picture, performed the task, and rated the strength of feeling (A). Brain

activity during Diminish trials (relative to View) showed significant time-point-by-condition interactions in somatosensory brain regions including right insula (B); brain regions that showed the intervention effect overlapped with regions that decreased activity during Diminish (relative to View) trials at baseline (pre-intervention; data from all available subjects shown for baseline in yellow, as reported in Min et al. (2022) (C); in addition, regions showing interaction effects corresponded with regions showing a decrease in activity during Diminish trials (relative to View) after the intervention in the Osc+ participants (D) but not with the occipital cluster showing a significant effect of time-point in Osc- participants (E). There were no effects of condition or time-point on ratings during Diminish (F) or View (G) trials. During Intensify trials, there was a main effect of time-point, with participants across conditions indicating stronger feelings in the post- than the pre-intervention scan (H).

As a manipulation check, we confirmed that the emotional pictures affected brain activity in emotion-related regions (including the amygdala) during view trials during the pre-intervention session (see Supplementary Fig. 5 and Supplementary Table 4). In analyses of the pre-intervention data (Min et al., 2022), we found that the brain regions targeted by attempting to diminish vs. intensify emotion were mostly non-overlapping. Thus, in our analyses, we separately compared condition effects during the Intensify trials and during the Diminish trials. We used the View condition as a baseline comparison for both.

ROI-based analyses revealed that pre-to-post change in left amygdala activity did not differ between conditions, $F(1, 82) = 0.001, p = 0.97, r = .00$ for Intensify > View, and $F(1, 82) = 2.17, p = 0.15, r = 0.16$ for View > Diminish (see Supplementary Table 4 for details). Also, pre-to-post change in right amygdala activity did not differ between conditions, $F(1, 82) = 0.94,$

$p = 0.34$, $r = .11$ for Intensify > View, and $F(1, 82) = 0.24$, $p = 0.63$, $r = .06$ for View > Diminish.

In whole-brain analyses, there were no significant interactions of condition by time-point for the Intensify > View contrasts. However, for the View > Diminish comparison, there was a significant interaction of time-point and condition in clusters within the right insula, central opercular cortex, parietal operculum cortex, postcentral gyrus, supramarginal gyrus, and superior parietal lobule (Fig. 5B). These regions that showed relatively less activity during Diminish than during View at post- than at pre-intervention overlapped with the regions suppressed (relative to View) during Diminish trials at baseline across all participants (Fig. 5C; baseline results from Min et al. (2022)). Comparison of post versus pre time-points for each group indicated that the time-point by condition interactions were driven by the Osc+ group who improved their ability to diminish brain activity in many interoceptive/sensory regions relative to View after the intervention (Fig. 5D). The only significant change across the five weeks in the Osc- group was in the occipital pole (Fig. 5E), but it was a cluster that did not overlap spatially with the condition-by-time-point interaction effect shown in Fig. 5B (see Supplementary Table 5 for the list of clusters). We also examined whether the intervention effect for the View > Diminish contrast differed between positive and negative emotion but did not find any significant differences.

The two conditions did not affect self-reported emotion regulation differentially.

Subjective ratings during the explicit regulation (Diminish and Intensify) trials did not show a significant interaction of time-point and condition, $p > .25$ for both conditions, but both groups rated pictures as more intense on Intensify trials after the intervention than before the

intervention, $F(1, 81) = 9.03, p = .004, r = .32$ (Figs. 5F, H). The interaction of time-point and condition for the View trials, $F(1,81) = 5.65, p = .02, r = .26$, did not quite meet the corrected significance level of 0.017 (Fig. 5G). This trend of interaction effect appeared to be due to both the Osc+ decrease, $p = 0.10$, and the Osc- increase, $p = 0.09$, in ratings of feeling strength during View trials after intervention, although the pairwise comparisons were not significant (see Supplementary Table 6 for details). Thus, the interventions did not differentially influence conscious emotion regulation.

The two daily biofeedback conditions affected subjective well-being similarly.

Self-rated mood became less negative across the course of the intervention (Supplementary Fig. 6A), with no significant difference in change between conditions. Self-rated anxiety showed no significant changes nor condition differences (Supplementary Fig. 6B), while scores on a depression scale showed improvements across the intervention in both conditions (Supplementary Fig. 6C). Most previous studies examining the effects of heart rate variability biofeedback have relied on no-intervention controls (Goessl et al., 2017); our findings highlight the importance of equating factors other than the critical physiological manipulations across conditions, as factors in the active intervention other than changes in heart rate variability may have an impact. One such factor influencing subjective ratings could be expectations. For both groups we framed the study as testing whether their biofeedback intervention would improve emotional well-being (e.g., Fig. 2A-B) and the two groups had similar expectations of improved well-being (Supplementary Fig. 2).

Breathing and other potential physiological confounds did not differ during target MRI scans across conditions.

There was not a significant time-point (Weeks 2 and 7) by condition interaction of breathing rates, heart rate, or HRV metrics during the resting-state fMRI scan, nor during the emotion-regulation task (see Supplementary Table 7 for means and statistical comparisons). In addition, during these two scans, neither exhaled carbon dioxide (CO₂) levels nor the average variability in CO₂ for the duration of the scan showed significant time-point by condition interactions. Likewise, a 2 (time-point: pre, post) X 2 (condition: Osc+, Osc-) ANOVA on whole-brain cerebral blood flow (CBF) during pseudo-continuous arterial spin labeling (pCASL) resting-state scans showed no significant effects.

In contrast with these lack of differences between conditions during rest and emotion regulation scans, we found significant differences in physiology in the ‘training-mimicking’ scan we conducted at the end of the session (see Supplementary Table 8). In terms of CBF, a 2 (scan type: pre-intervention rest, post-intervention training mimicking) X 2 (condition: Osc+, Osc-) ANOVA yielded a significant main effect of scan type, $F(1,51) = 9.48, p = .003, r = .40$, as CBF was lower during training mimicking ($M = 39.33, SE = 1.08, SD = 7.88$) than during rest ($M = 42.45, SE = 1.14, SD = 8.32$) across conditions. There was no significant main effect of condition, $F(1,51) = .91, p = .35, r = .14$, and the interaction of scan type and condition was not significant, $F(1,51) = 1.30, p = .26, r = .17$. In summary, the two conditions had significant effects on breathing, CO₂, and HRV during training that did not carry over to the target scan sessions where we assessed emotion-related brain activity during rest and during emotion regulation.

Discussion

Our study followed up on intriguing findings suggesting that HRV biofeedback improves well-being (Goessl et al., 2017; Lehrer & Gevirtz, 2014; Mather & Thayer, 2018; Pizzoli et al., 2021) to test the hypothesis that experiencing daily sessions involving increased heart rate oscillation (the Osc+ intervention) would affect resting-state functional connectivity within emotion networks. We also examined whether the Osc+ intervention would influence the responsiveness to emotion regulation attempts in brain regions involved in emotional experience. The Osc+ intervention increased the amplitude of heart rate oscillation via slow paced breathing at approximately the frequency of the baroreflex, creating resonance (Lehrer & Gevirtz, 2014). Previous findings indicate increases in heart rate oscillatory amplitude during resonance breathing are vagally mediated (Kromenacker et al., 2018).

When planning this study, we selected changes in right amygdala-mPFC functional connectivity as our primary outcome measure because of our prior observation that right amygdala-mPFC functional connectivity was associated with HRV (Sakaki et al., 2016); we were interested in whether HRV plays a causal role in increasing functional connectivity within this circuit. In the current study, spending 20-40 minutes/day in a high physiological oscillatory state for a few weeks had no significant effect on right amygdala-mPFC connectivity, thus failing to confirm our main hypothesis. However, this intervention did increase left amygdala-mPFC functional connectivity. A prior meta-analysis identified the left (but not right) amygdala as showing activity related to HRV (Thayer et al., 2012) and our prior study examining the relationship of how amygdala functional connectivity relates to individual differences in HRV found that, in younger adults, both left and right amygdala connectivity with ventrolateral PFC

was related to HRV (Sakaki et al., 2016). Thus, prior studies have identified both right and left amygdala functional connectivity relationships with HRV.

In a recent review, we proposed that daily time spent stimulating physiological oscillatory activity should increase chronic levels of oscillatory activity in emotion-related resting-state brain networks (Mather & Thayer, 2018). Indeed, our analyses examining the broader context of functional connectivity within canonical resting-state networks indicate that the functional connectivity changes seen in the left amygdala are not unique; instead, they are part of a general pattern in our study of increased functional connectivity in emotion-related networks in the Osc+ condition, an increase in functional connectivity that is greater than in non-emotion networks. As detailed in the methods section, these emotion-related networks are associated with a wide range of emotional and autonomic processes. In particular, the emotion networks that Osc+ participants showed most pronounced change in involve interoceptive processing. Thus, the current findings support our hypothesis that inducing large oscillations in heart rate leads to increased functional connectivity within brain networks that respond to interoceptive input and help shape emotions. Although self-rated emotional well-being and emotion regulation effectiveness was not differentially affected in this healthy sample, future work is needed to test whether increasing resting-state functional connectivity in emotion-related networks can benefit patients with affective disorders.

One of our secondary outcomes examined whether the intervention would influence participants' ability to up- or down-regulate amygdala activity on demand. There were no significant effects of the intervention on amygdala activity during emotion regulation. However, when we examined whole-brain activity we found that the Osc+ intervention led to more effective down-regulation of brain regions associated with sensing body states when attempting

to regulate emotional responses to pictures. Thus, the Osc+ intervention affected both resting state functional connectivity and task-related activity in brain regions associated with emotional and interoceptive processes.

A prior meta-analysis suggested that, during reappraisal of negative stimuli, patients with mood and anxiety disorders show more activity in a set of brain regions that overlaps regions that Osc+ participants were better able to down-regulate after the intervention, including the right posterior insula, right inferior and superior parietal lobule, right postcentral gyrus, and right operculum (Picó-Pérez et al., 2017). These brain regions process signals from the body. Large oscillations in heart rate may strengthen feedback loops involving these brain regions, making these feedback loops more responsive during emotion regulation attempts and increasing participants' ability to down-regulate activity in these brain regions that not only sense body states, but also simulate them, such as when viewing pictures of others (Keysers et al., 2010). Our findings suggest that daily practice increasing heart rate oscillatory activity improved participants' ability to diminish activity in brain regions involved in feeling emotional body states when they wanted to minimize their emotional reactions to stimuli.

These findings not only demonstrate that daily sessions involving high heart rate oscillatory activity affect subsequent brain activity in emotion-related brain regions, but also have implications for models of emotion regulation. There are different models of how cognitive appraisal (the strategy used by most participants in our study) affects amygdala activity. In one model, cognitive control regions (i.e., dorsolateral, ventrolateral and ventrolateral subregions of PFC and posterior parietal cortex) engage ventromedial PFC (vmPFC), which via its anatomical connectivity with the amygdala relays the control messages (Buhle et al., 2014). This model guided our initial hypothesis that increased functional connectivity between mPFC and amygdala

would increase Osc+ participants' ability to regulate amygdala activity. However, in another model, prefrontal and parietal control regions affect amygdala by altering semantic and perceptual representations in lateral temporal areas when reappraising stimuli (Buhle et al., 2014). Meta-analyses of emotion regulation studies support the latter model in which conscious reappraisal does not rely on vmPFC to influence amygdala activity (Berboth & Morawetz, 2021; Buhle et al., 2014). Instead, the vmPFC may influence the amygdala more during implicit emotion regulation processes (Sakaki et al., 2016). If the vmPFC is not engaged in the reappraisal process, this could explain how the Osc+ intervention could increase amygdala-mPFC functional connectivity during rest but not enhance modulation of amygdala activity during reappraisal. Thus, our findings support the notion that mPFC has little impact on the amygdala during explicit emotion regulation.

If amygdala-mPFC functional connectivity has little impact on explicit emotion regulation, why is it so often disrupted in various disorders involving disordered emotion regulation, such as anxiety, bipolar disorder, and posttraumatic stress disorder (Chepenik et al., 2010; Hamm et al., 2014; Sripada et al., 2012; Stevens et al., 2013)? Implicit emotion regulation processes also play a key role in well-being (Braunstein et al., 2017). For instance, the ability to learn through experience that a conditioned stimulus is no longer associated with an unconditioned stimulus (extinction, a type of implicit emotion regulation) is impaired in PTSD and other disorders. In rodents, vagal nerve stimulation enhances extinction learning and plasticity in the amygdala-mPFC pathway (Childs et al., 2017; Peña et al., 2014). One possibility that should be examined in future research is that the intervention affects implicit rather than explicit emotion regulation processes.

While the Osc+ intervention did not affect the ability to down-regulate the amygdala during explicit emotion regulation, it did increase down-regulation of activity in brain regions associated with sensing somatic states. In a separate report (Min et al., 2022), we compared brain activity during “intensify” and “diminish” emotion regulation trials across all participants in the pre-intervention session. We were guided by the hypothesis that regulatory control regions act like an affective dial, turning up activity in emotion-related regions when people attempt to intensify emotions while turning down activity in those same regions when people attempt to diminish emotions. This affective dial hypothesis had been implicitly assumed by emotion regulation researchers (including us) but had not been explicitly tested. To our surprise, intensifying and diminishing emotions targeted different brain regions, with diminishing emotions decreasing brain activity in interoceptive/somatosensory brain regions and intensifying emotions increasing activity in other emotion-related regions. This dissociation is also reflected in the intervention results, as the Osc+ intervention affected brain activity during diminishing emotions but not during intensifying emotions.

Prior work comparing up- vs. down-regulating emotions has focused on the common control regions tapped by these processes and has not addressed the question of whether these regulatory control processes target activity in different emotion-related brain regions (Morawetz et al., 2017). The different emotion-related brain regions targeted by Diminish and Intensify conditions in our baseline data (Min et al., 2022) and the finding that the Osc+ intervention increased the ability to down-regulate activity in the emotion-related brain regions targeted during Diminish trials but had no effect on the emotion-related brain regions targeted during Intensify trials argue against the field’s implicit “affective dial hypothesis” in which up- and down-regulation have opposing effects on the same emotion-related brain regions. Furthermore,

they suggest that some interventions (like the Osc+ intervention) may be more effective for modulating down-regulation processes, whereas other interventions may be more effective for modulating up-regulation processes.

BOLD MRI signal is influenced by breathing and by CO₂ levels, thus one obvious question is whether the condition differences in change in brain activity were mediated by participants in the Osc+ condition breathing more slowly even when not engaged in a training session. This does not appear to be the case, as there were no significant differences between the Osc+ and Osc- conditions in breathing rates during the resting-state or emotion regulation scans. Heart rate, HRV, end-tidal CO₂, and blood flow also did not differ significantly during these scans (although LF-HRV during seated rest increased among the Osc+ participants; see Supplementary Fig. 7). In any case, the condition differences were not the result of a global change in BOLD signal, as we found that the Osc+ condition increased functional connectivity in emotion-related networks more than in other resting-state networks and the Osc+ intervention strengthened ability to down-regulate interoception-related brain activity specifically when trying to diminish emotions. In addition, our multi-echo fMRI scan processing pipeline helped avoid common confounding signal artifacts from the basal vein of Rosenthal in our amygdala connectivity analyses (see Supplementary Fig. 4).

One of the unique strengths of our study compared to most previous HRV-biofeedback studies was the active comparison group (Osc-) who completed an intervention resembling the target Osc+ intervention, but with minimal effects on HRV (see Fig. 2). We found that participants in both conditions showed significant decreases in negative mood states and in depression scores. Thus, the active comparison group was important in revealing that some aspects of the biofeedback protocol other than its effects on HRV were associated with improved

emotional well-being. One possibility is that spending time every day in an awake quiet restful state yields emotional benefits regardless of whether the relaxing state increases physiological oscillatory activity. Another is that participants' expectations (which were similarly positive in the two conditions) led to the improvements in self-reported emotional states. It is also possible that the CES-D is not the best depression scale to assess HRV biofeedback effects (Pizzoli et al., 2021). In any case, these findings point to the importance of including active comparison groups with matched expectations in research examining the effects of behavioral interventions on well-being (Davidson & Kaszniak, 2015).

Across both conditions, more than half of the participants in our study were Asian. We recruited on campus; our Asian student overrepresentation may reflect ethnic differences in interest in participating in a study related to heart rate biofeedback and meditation. As Asians and European Americans differ in their ideal affect (Tsai et al., 2006) and cardiovascular physiology differs between African Americans and European Americans (Brownlow et al., 2020), future studies should examine whether heart rate variability biofeedback effects differ by ethnicity.

In conclusion, we found that, in young healthy adults, daily sessions involving high amplitude heart rate oscillations affected emotion-related brain activity both when resting and when diminishing emotional responses. Repeated large heart-rate increases/decreases during biofeedback sessions provide a powerful physiological input that may act as a "workout" for cortical regions involved in physiological control, enhancing the brain's capacity to respond in goal-consistent ways when later confronted with emotional stimuli.

Open Practices Statement

This study was preregistered prior to conducting research (Heart Rate Variability and Emotion Regulation or “HRV-ER” at <https://clinicaltrials.gov/ct2/show/NCT03458910>). Upon publication, data associated with this study will be made publicly available at <https://openneuro.org/datasets/ds003823>.

References

- Banks, S. J., Eddy, K. T., Angstadt, M., Nathan, P. J., & Phan, K. L. (2007). Amygdala–frontal connectivity during emotion regulation. *Social Cognitive and Affective Neuroscience*, *2*(4), 303-312.
- Beauchaine, T. P., & Thayer, J. F. (2015). Heart rate variability as a transdiagnostic biomarker of psychopathology. *International Journal of Psychophysiology*, *98*(2), 338-350.
- Bechara, A., & Damasio, A. R. (2005). The somatic marker hypothesis: A neural theory of economic decision. *Games and Economic Behavior*, *52*(2), 336-372. [<Go to ISI>://000231182200007](#)
- Berboth, S., & Morawetz, C. (2021). Amygdala–prefrontal connectivity during emotion regulation: A meta-analysis of psychophysiological interactions. *Neuropsychologia*, *153*, 107767.
- Bernardi, L., Sleight, P., Bandinelli, G., Cencetti, S., Fattorini, L., Wdowczyk-Szulc, J., & Lagi, A. (2001). Effect of rosary prayer and yoga mantras on autonomic cardiovascular rhythms: comparative study. *BMJ*, *323*(7327), 1446-1449. <https://doi.org/10.1136/bmj.323.7327.1446>
- Boubela, R. N., Kalcher, K., Huf, W., Seidel, E.-M., Derntl, B., Pezawas, L., Našel, C., & Moser, E. (2015). fMRI measurements of amygdala activation are confounded by stimulus correlated signal fluctuation in nearby veins draining distant brain regions. *Scientific Reports*, *5*(1), 10499. <https://doi.org/10.1038/srep10499>
- Braunstein, L. M., Gross, J. J., & Ochsner, K. N. (2017). Explicit and implicit emotion regulation: a multi-level framework. *Social Cognitive and Affective Neuroscience*, *12*(10), 1545-1557.
- Brownlow, B. N., Williams, D., Kapuku, G., Vasey, M. W., Anderson, N. B., Koenig, J., Thayer, J. F., & Hill, L. (2020). Ethnic Differences in Resting Total Peripheral Resistance: A Systematic Review and Meta-Analysis. *Psychosomatic Medicine*.
- Buhle, J. T., Silvers, J. A., Wager, T. D., Lopez, R., Onyemekwu, C., Kober, H., Weber, J., & Ochsner, K. N. (2014). Cognitive reappraisal of emotion: a meta-analysis of human neuroimaging studies. *Cerebral Cortex*, *24*(11), 2981-2990.
- Chen, Y., Wang, D. J., & Detre, J. A. (2011). Test–retest reliability of arterial spin labeling with common labeling strategies. *Journal of Magnetic Resonance Imaging*, *33*(4), 940-949.
- Chepenik, L. G., Raffo, M., Hampson, M., Lacadie, C., Wang, F., Jones, M. M., Pittman, B., Skudlarski, P., & Blumberg, H. P. (2010). Functional connectivity between ventral prefrontal cortex and amygdala at low frequency in the resting state in bipolar disorder. *Psychiatry Research: Neuroimaging*, *182*(3), 207-210. <https://doi.org/https://doi.org/10.1016/j.psychresns.2010.04.002>
- Childs, J. E., DeLeon, J., Nickel, E., & Kroener, S. (2017). Vagus nerve stimulation reduces cocaine seeking and alters plasticity in the extinction network. *Learning and Memory*, *24*(1), 35-42.
- Damasio, A., & Carvalho, G. B. (2013). The nature of feelings: evolutionary and neurobiological origins. *Nature Reviews Neuroscience*, *14*(2), 143.
- Davidson, R. J., & Kaszniak, A. W. (2015). Conceptual and methodological issues in research on mindfulness and meditation. *American Psychologist*, *70*(7), 581.
- Dipasquale, O., Sethi, A., Laganà, M. M., Baglio, F., Baselli, G., Kundu, P., Harrison, N. A., & Cercignani, M. (2017). Comparing resting state fMRI de-noising approaches using multi-and single-echo acquisitions. *Plos One*, *12*(3).

- Fischl, B., Van Der Kouwe, A., Destrieux, C., Halgren, E., Ségonne, F., Salat, D. H., Busa, E., Seidman, L. J., Goldstein, J., & Kennedy, D. (2004). Automatically parcellating the human cerebral cortex. *Cerebral Cortex*, *14*(1), 11-22.
- Geisler, F. C., Vennewald, N., Kubiak, T., & Weber, H. (2010). The impact of heart rate variability on subjective well-being is mediated by emotion regulation. *Personality and Individual Differences*, *49*(7), 723-728.
- Goessl, V., Curtiss, J., & Hofmann, S. (2017). The effect of heart rate variability biofeedback training on stress and anxiety: a meta-analysis. *Psychological Medicine*, 1-9.
- Hagemann, D., Waldstein, S. R., & Thayer, J. F. (2003). Central and autonomic nervous system integration in emotion. *Brain and Cognition*, *52*(1), 79-87.
- Hamm, L. L., Jacobs, R. H., Johnson, M. W., Fitzgerald, D. A., Fitzgerald, K. D., Langenecker, S. A., Monk, C. S., & Phan, K. L. (2014). Aberrant amygdala functional connectivity at rest in pediatric anxiety disorders. *Biology of Mood & Anxiety Disorders*, *4*(1), 15.
<https://doi.org/10.1186/s13587-014-0015-4>
- Heartmath. (2016). *EmWave Pro Plus*. In <https://store.heartmath.com/emwave-pro-plus/>
- Jenkinson, M., Beckmann, C. F., Behrens, T. E., Woolrich, M. W., & Smith, S. M. (2012). Fsl. *Neuroimage*, *62*(2), 782-790.
- Kemp, A. H., & Quintana, D. S. (2013). The relationship between mental and physical health: Insights from the study of heart rate variability. *International Journal of Psychophysiology*, *89*(3), 288-296. <https://doi.org/https://doi.org/10.1016/j.ijpsycho.2013.06.018>
- Keysers, C., Kaas, J. H., & Gazzola, V. (2010). Somatosensation in social perception. *Nature Reviews Neuroscience*, *11*(6), 417-428.
- Kim, S. H., & Hamann, S. (2007). Neural correlates of positive and negative emotion regulation. *Journal of Cognitive Neuroscience*, *19*(5), 776-798.
- Koenig, J., Abler, B., Agartz, I., Åkerstedt, T., Andreassen, O. A., Anthony, M., Bär, K. J., Bertsch, K., Brown, R. C., & Brunner, R. (2021). Cortical thickness and resting-state cardiac function across the lifespan: A cross-sectional pooled mega-analysis. *Psychophysiology*, *58*(7), e13688.
- Kromenacker, B. W., Sanova, A. A., Marcus, F. I., Allen, J. J., & Lane, R. D. (2018). Vagal mediation of low-frequency heart rate variability during slow yogic breathing. *Psychosomatic Medicine*, *80*(6), 581-587.
- Kundu, P., Brenowitz, N. D., Voon, V., Worbe, Y., Vértes, P. E., Inati, S. J., Saad, Z. S., Bandettini, P. A., & Bullmore, E. T. (2013). Integrated strategy for improving functional connectivity mapping using multiecho fMRI. *Proceedings of the National Academy of Sciences*, *110*(40), 16187-16192.
- Kundu, P., Inati, S. J., Evans, J. W., Luh, W.-M., & Bandettini, P. A. (2012). Differentiating BOLD and non-BOLD signals in fMRI time series using multi-echo EPI. *Neuroimage*, *60*(3), 1759-1770.
- Kundu, P., Voon, V., Balchandani, P., Lombardo, M. V., Poser, B. A., & Bandettini, P. A. (2017). Multi-echo fMRI: A review of applications in fMRI denoising and analysis of BOLD signals. *Neuroimage*, *154*, 59-80. <https://doi.org/https://doi.org/10.1016/j.neuroimage.2017.03.033>
- Laird, A. R., Fox, P. M., Eickhoff, S. B., Turner, J. A., Ray, K. L., McKay, D. R., Glahn, D. C., Beckmann, C. F., Smith, S. M., & Fox, P. T. (2011). Behavioral interpretations of intrinsic connectivity networks. *Journal of Cognitive Neuroscience*, *23*(12), 4022-4037.

- Lee, H., Heller, A. S., Van Reekum, C. M., Nelson, B., & Davidson, R. J. (2012). Amygdala–prefrontal coupling underlies individual differences in emotion regulation. *Neuroimage*, *62*(3), 1575-1581.
- Lehrer, P., Sasaki, Y., & Saito, Y. (1999). Zazen and cardiac variability. *Psychosomatic Medicine*, *61*(6), 812-821.
- Lehrer, P., Vaschillo, B., Zucker, T., Graves, J., Katsamanis, M., Aviles, M., & Wamboldt, F. (2013). Protocol for heart rate variability biofeedback training. *Biofeedback*, *41*(3), 98-109.
- Lehrer, P. M., & Gevirtz, R. (2014). Heart rate variability biofeedback: how and why does it work? *Frontiers in psychology*, *5*, 756.
- Lynch, C. J., Power, J. D., Scult, M. A., Dubin, M., Gunning, F. M., & Liston, C. (2020). Rapid precision functional mapping of individuals using multi-echo fMRI. *Cell reports*, *33*(12), 108540.
- Mather, M., & Thayer, J. F. (2018). How heart rate variability affects emotion regulation brain networks. *Current Opinion in Behavioral Sciences*, *19*, 98-104.
- McCraty, R., Atkinson, M., Tomasino, D., & Bradley, R. T. (2009). The coherent heart heart-brain interactions, psychophysiological coherence, and the emergence of system-wide order. *Integral Review: A Transdisciplinary & Transcultural Journal for New Thought, Research, & Praxis*, *5*(2).
- Min, J., Nashiro, K., Yoo, H. J., Cho, C., Nasser, P., Bachman, S. L., Porat, S., Thayer, J. F., Chang, C., & Lee, T.-H. (2022). Emotion Downregulation Targets Interoceptive Brain Regions While Emotion Upregulation Targets Other Affective Brain Regions. *Journal of Neuroscience*, *42*(14), 2973-2985.
- Monfredi, O., Dobrzynski, H., Mondal, T., Boyett, M. R., & Morris, G. M. (2010). The anatomy and physiology of the sinoatrial node—a contemporary review. *Pacing and Clinical Electrophysiology*, *33*(11), 1392-1406.
- Morawetz, C., Bode, S., Derntl, B., & Heekeren, H. R. (2017). The effect of strategies, goals and stimulus material on the neural mechanisms of emotion regulation: A meta-analysis of fMRI studies. *Neuroscience and Biobehavioral Reviews*, *72*, 111-128.
- Nickerson, L. D., Smith, S. M., Öngür, D., & Beckmann, C. F. (2017). Using dual regression to investigate network shape and amplitude in functional connectivity analyses. *Frontiers in Neuroscience*, *11*, 115.
- Peña, D. F., Childs, J. E., Willett, S., Vital, A., McIntyre, C. K., & Kroener, S. (2014). Vagus nerve stimulation enhances extinction of conditioned fear and modulates plasticity in the pathway from the ventromedial prefrontal cortex to the amygdala. *Frontiers in Behavioral Neuroscience*, *8*, 327.
- Peng, C. K., Henry, I. C., Mietus, J. E., Hausdorff, J. M., Khalsa, G., Benson, H., & Goldberger, A. L. (2004). Heart rate dynamics during three forms of meditation. *International Journal of Cardiology*, *95*(1), 19-27. <https://doi.org/http://dx.doi.org/10.1016/j.ijcard.2003.02.006>
- Peng, C. K., Mietus, J. E., Liu, Y., Khalsa, G., Douglas, P. S., Benson, H., & Goldberger, A. L. (1999). Exaggerated heart rate oscillations during two meditation techniques. *International Journal of Cardiology*, *70*(2), 101-107.
- Picó-Pérez, M., Radua, J., Steward, T., Menchón, J. M., & Soriano-Mas, C. (2017). Emotion regulation in mood and anxiety disorders: a meta-analysis of fMRI cognitive reappraisal studies. *Progress in Neuro-Psychopharmacology and Biological Psychiatry*, *79*, 96-104.

- Pizzoli, S. F., Marzorati, C., Gatti, D., Monzani, D., Mazzocco, K., & Pravettoni, G. (2021). A meta-analysis on heart rate variability biofeedback and depressive symptoms. *Scientific Reports*, *11*(1), 1-10.
- Poppa, T., & Bechara, A. (2018). The somatic marker hypothesis: revisiting the role of the 'body-loop' in decision-making. *Current Opinion in Behavioral Sciences*, *19*, 61-66.
- Reyes del Paso, G. A., Langewitz, W., Mulder, L. J., Roon, A., & Duschek, S. (2013). The utility of low frequency heart rate variability as an index of sympathetic cardiac tone: a review with emphasis on a reanalysis of previous studies. *Psychophysiology*, *50*(5), 477-487.
- Sakaki, M., Yoo, H. J., Nga, L., Lee, T.-H., Thayer, J. F., & Mather, M. (2016). Heart rate variability is associated with amygdala functional connectivity with MPFC across younger and older adults. *Neuroimage*, *139*, 44-52.
- Sarmiento, S., García-Manso, J. M., Martín-González, J. M., Vaamonde, D., Calderón, J., & Da Silva-Grigoletto, M. E. (2013). Heart rate variability during high-intensity exercise. *Journal of Systems Science and Complexity*, *26*(1), 104-116.
- Smith, R., Thayer, J. F., Khalsa, S. S., & Lane, R. D. (2017). The hierarchical basis of neurovisceral integration. *Neuroscience and Biobehavioral Reviews*, *75*, 274-296.
- Smith, S. M., & Nichols, T. E. (2009). Threshold-free cluster enhancement: addressing problems of smoothing, threshold dependence and localisation in cluster inference. *Neuroimage*, *44*(1), 83-98.
- Sripada, R. K., King, A. P., Garfinkel, S. N., Wang, X., Sripada, C. S., Welsh, R. C., & Liberzon, I. (2012). Altered resting-state amygdala functional connectivity in men with posttraumatic stress disorder. *Journal of Psychiatry and Neuroscience*, *37*(4), 241-249.
- Stevens, J. S., Jovanovic, T., Fani, N., Ely, T. D., Glover, E. M., Bradley, B., & Ressler, K. J. (2013). Disrupted amygdala-prefrontal functional connectivity in civilian women with posttraumatic stress disorder. *Journal of Psychiatric Research*, *47*(10), 1469-1478.
<https://doi.org/https://doi.org/10.1016/j.jpsychires.2013.05.031>
- Tarvainen, M. P., Niskanen, J.-P., Lipponen, J. A., Ranta-Aho, P. O., & Karjalainen, P. A. (2014). Kubios HRV—heart rate variability analysis software. *Computer Methods and Programs in Biomedicine*, *113*(1), 210-220.
- Terathongkum, S., & Pickler, R. H. (2004). Relationships among heart rate variability, hypertension, and relaxation techniques. *Journal of Vascular Nursing*, *22*(3), 78-82.
- Thayer, J. F., Åhs, F., Fredrikson, M., Sollers, J. J., & Wager, T. D. (2012). A meta-analysis of heart rate variability and neuroimaging studies: implications for heart rate variability as a marker of stress and health. *Neuroscience and Biobehavioral Reviews*, *36*(2), 747-756.
- Thayer, J. F., & Lane, R. D. (2009). Claude Bernard and the heart–brain connection: Further elaboration of a model of neurovisceral integration. *Neuroscience and Biobehavioral Reviews*, *33*(2), 81-88.
- Tsai, J. L., Knutson, B., & Fung, H. H. (2006). Cultural variation in affect valuation. *Journal of Personality and Social Psychology*, *90*(2), 288.
- van Osch, M. J., Teeuwisse, W. M., van Walderveen, M. A., Hendrikse, J., Kies, D. A., & van Buchem, M. A. (2009). Can arterial spin labeling detect white matter perfusion signal? *Magnetic Resonance in Medicine: An Official Journal of the International Society for Magnetic Resonance in Medicine*, *62*(1), 165-173.

- Wang, Z., Aguirre, G. K., Rao, H., Wang, J., Fernandez-Seara, M. A., Childress, A. R., & Detre, J. A. (2008). Empirical optimization of ASL data analysis using an ASL data processing toolbox: ASLtbx. *Magnetic Resonance Imaging*, *26*(2), 261-269. <Go to ISI>://000253225700014
- Yoo, H. J., Thayer, J. F., Greening, S. G., Lee, T. H., Ponzio, A., Min, J., Sakaki, M., Nga, L., Mather, M., & Koenig, J. (2018). Brain structural concomitants of resting state heart rate variability in the young and old: Evidence from two independent samples. *Brain Structure & Function*, *223*, 727-737.

Funding

This study was supported by NIH R01AG057184 (PI Mather).

Acknowledgments

This study was supported by NIH R01AG057184 (PI Mather). We thank our research assistants for their help with data collection: Michelle Wong, Kathryn Cassutt, Collin Amano, Yong Zhang, Paul Choi, Heekyung Rachael Kim, Seungyeon Lee, Alexandra Haydinger, Lauren Thompson, Gabriel Shih, Divya Suri, Sophia Ling, Akanksha Jain, and Linette Bagtas.

Contributions

K.N., J.M., and H.Y. equally contributed to the manuscript and are co-first authors. M.M. conceptualized the study, designed the study with the input from J.F.T., P.L., and C. Chang, and analyzed the data. K.N. helped design the study, directed the research team, collected and analyzed the data. J.M. and H.Y. helped with the initial setup and design of the study, collected and analyzed the data. Data collection was also performed by C. Cho with the assistance of S.L.B., P.N. and D.W. C. Cho, S.L.B. and S.D. also analyzed the data. J.F.T., P.L., C. Chang, D.A.N. and V.Z.M. provided technical assistance with data acquisition and analyses and helped interpret the results. With the supervision of S.N., T.F. developed a customized app for the Osc-training group and contributed to data management. N.M. developed a customized app for participants to track their training progress and contributed to data management. All authors contributed to manuscript preparation.

Conflict of interest

The authors declare no competing interests.

Supplementary Materials

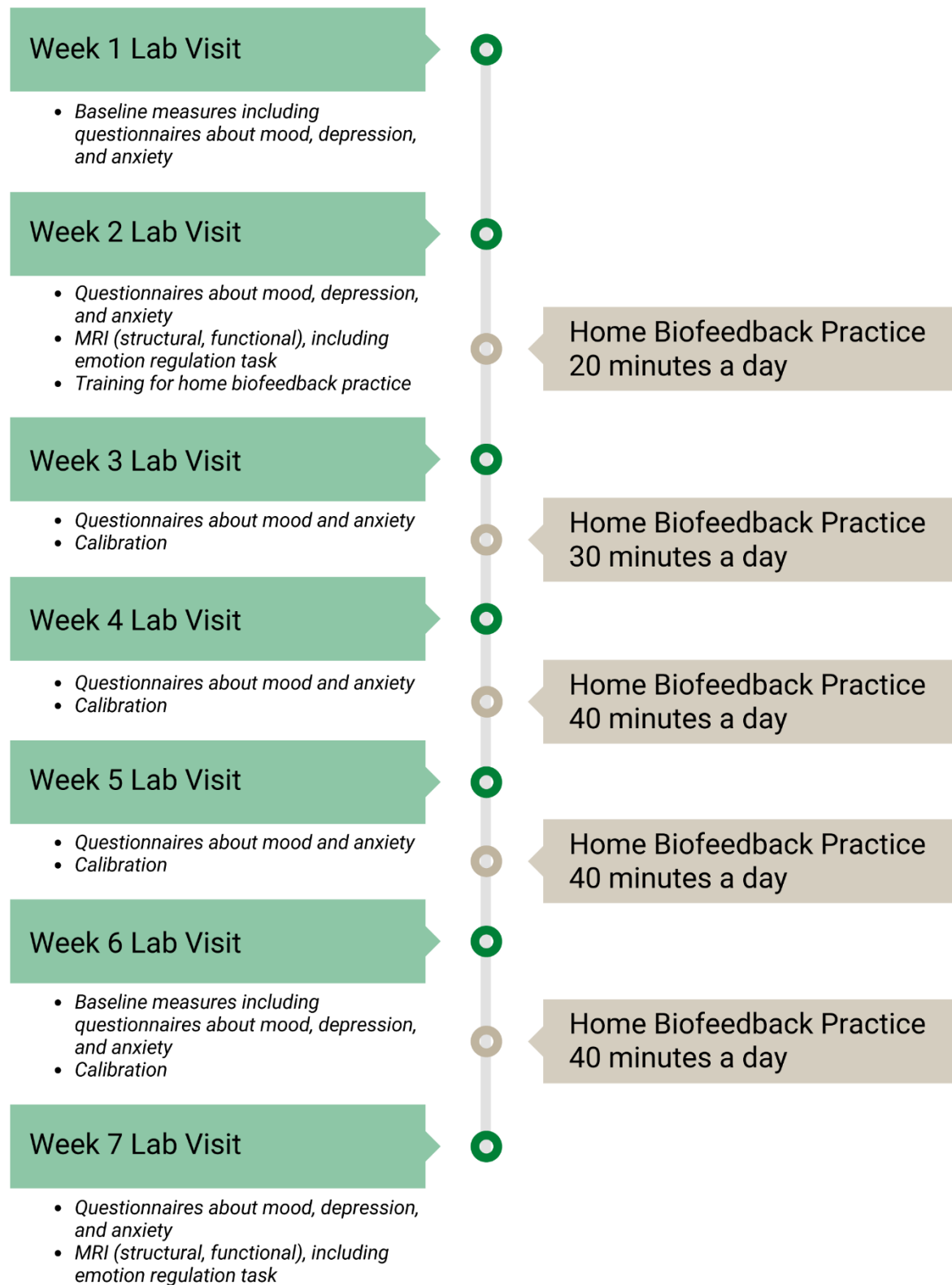
Supplementary Methods

Power Considerations

No prior studies had examined effects of these interventions on brain function so we were unable to estimate effect sizes based on prior neuroimaging data. We elected to power our study to detect medium or larger effect sizes. Our main planned statistical comparisons were repeated-measures ANOVAs with within-between interactions. For these, a total sample size of 46 would give 90% power to detect moderate effect sizes of $f = .25$ with $\alpha = .05$, given an assumed correlation among the repeated measures of .5 (Faul et al., 2007). We also planned to examine within-subject change within each of the conditions. A sample size of 44 in each group would give 90% power to detect within-group change effect sizes of $d = .5$ in a two-tailed t-test with $\alpha = .05$ (Faul et al., 2007). Thus, we aimed for an $N = 100$ completion rate across the two groups to be able to accommodate potential exclusions for movement during imaging or other data quality issues. Supplementary Figure 1 details how many participants we were able to include for each category of data.

Supplementary Figure 1

7-week study schedule: Lab visits and biofeedback training



Randomization

Participants were assigned to small groups of 3-6 people, with each group meeting at the same time and day each week. Group assignment was based on their availability (e.g., people who are available on Mondays for each week were assigned to the Monday group). After recruitment and scheduling of each wave of groups were complete, two full-time researchers generated the random assignment using flipping a coin method and assigned groups of participants to one of the two conditions. Participants were not informed which intervention was the 'target' intervention. All participants were told that they would be assigned to one of the two types of heart rate biofeedback training and that the study investigates the effect of each training on emotional well-being and associated brain function. All researchers were blind to condition assignment until a few days before the participant's first visit.

Osc- Condition

As described in the main text, we wanted to avoid having participants figure out that one way to reduce their HRV and get positive feedback would be to do something like get up and do jumping jacks (physical activity typically decreases HRV (Sarmiento et al., 2013)). Thus, we told Osc- participants to try to lower their heart rate in addition to lowering their heart rate oscillations and we intended to build into the feedback a minor point penalty when heart rate was the highest it had been in a short while. However, due to a coding error not detected until the study was over, this point adjustment did the opposite, giving a penalty when heart rate was the lowest it had been in the most recent 15 s. Specifically, every 5 s, a local maximum IBI was set based on the maximum IBI from the past 15 s. If, at that point, the participant's current IBI was longer than this local maximum, the calmness score displayed for the next 5 s was the anti-coherence score - 2. Naturally, most of the time, current IBI was lower than the local maximum,

and in those cases, the calmness score was the anti-coherence score +1. Thus, there was a penalty in their calmness score for moments when their heart rate was slower than it had been in any of the past 15 s. As reported in the results, average heart rate during biofeedback sessions did not differ significantly across conditions. Thus, this additional feedback appeared to have had little impact on heart rate, consistent with prior findings that biofeedback to increase or decrease heart rate has no significant impact (Bennett et al., 1978).

Post-Study Questionnaire

After the Week-7 post-intervention scan, participants completed a questionnaire surveying their experience during the study. They provided self-ratings of difficulty of daily heart rate biofeedback training, level of effort to complete the training, expectations of the training impact on well-being, and likelihood of continuing the training after the study's conclusion.

Emotion Regulation Task

Participants were instructed to intensify or diminish the emotional arousal the picture elicited (whether positive or negative), or to just view it. We asked participants to come up with their own methods to accomplish these emotion regulation goals. If participants had a hard time doing so during practice trials, we provided them with examples such as reinterpreting the situations in the image and adjusting the distance between the objects in the picture and themselves. We also instructed them not to generate an emotion opposite to the one they were experiencing. For example, they were not supposed to substitute a positive emotion for a negative one to moderate their emotion. After MRI scans, we had participants rate their confidence in accomplishing the four emotion regulation conditions (i.e., diminish-negative,

diminish-positive, intensify-negative, intensify-positive) and report their emotion regulation strategies.

Trials from each condition were nested in groups of three within mini-blocks. A fixation cross with a jittering interval separated the same-condition events within each block such that two jittering intervals summed up to 4s. The blocks were separated by 5-s inter-block intervals, during which a fixation cross was displayed. This resulted in 14 blocks and 42 event-related trials in total. The blocks were presented in a pseudo-random manner such that no blocks with identical instruction nor blocks with same-valence images were presented consecutively. We selected six counterbalanced sets of 18 positive, 18 negative, and 6 neutral images from the International Affective Picture System (Lang et al., 1999) such that within each of the six sets, each picture valence type subset had the same average valence and arousal scores (positive images: mean valence = 7.2, mean arousal = 5.4; negative images: mean valence = 2.8, mean arousal = 5.4; neutral images: mean valence = 5.0, mean arousal = 2.8). Each participant was presented with one of these sets during the task scan before training and a different set after training.

Weekly Questionnaires

During each lab visit, participants completed the profile of mood states (POMS; Grove & Prapavessis, 1992) and the state anxiety inventory (SAI; Spielberger & Gorsuch, 1983). We used the 40-item version of POMS. Participants reported how much each item reflected how they felt at the moment using a scale from 1 (not at all) to 5 (extremely). Total mood disturbance was calculated by subtracting positive-item totals from negative-item totals. A constant value (i.e., 100) was added to the total mood disturbance to eliminate negative scores. Higher scores indicate greater negative affect. The SAI measures state anxiety using 20 statements. Participants

indicated how they felt at the moment on a scale from 1 (not at all) to 4 (very much so). Scores range between 20 and 80 and higher scores indicate greater anxiety. We also administered the Center for Epidemiological Studies Depression Scale (CES-D; Radloff, 1977) in Weeks 1, 2, 6 and 7. Positive scores indicate greater symptoms of depression.

Compensation and Rewards for Performance

Upon completing the study, participants received compensation of \$15 per hour for each lab visit. Participants were also eligible to receive rewards based on individual and group performance (incentives for training were the same across conditions). For individual performance rewards, each week participants had the opportunity to earn \$2 for each instance (up to a maximum of 10) they exceeded their assigned target score (target scores were assigned each week and were the average of the top 10 scores earned from the previous week's training sessions plus 0.3). Group performance rewards were earned when members of a participant's group completed a minimum of 80% of their assigned biofeedback training minutes. For example, if a participant completed 100% of their training, they received an additional \$3 for each group member who also completed 100% of their training. If a participant completed 80% of their training, they received an additional \$2 for each group member who also completed at least 80% of their training. Rewards were calculated weekly, and participants received weekly updates on their earnings at their lab visit.

Analyses

Heart Rate Oscillations During Training

Heart rate data from ear sensors failed to save for the first four participants in the Osc-condition because of technical issues with the first version of the Osc- biofeedback software,

leaving 102 participants' data across the two conditions (5827 sessions). We averaged the autoregressive total spectral power from all training sessions for each participant. We excluded five outliers who on a box-and-whisker plot were above $Q3 + 3 * \text{the interquartile range}$ on total power on pre-intervention rest ($N=3$), post-intervention rest ($N=1$), or average training ($N=1$), leaving an N of 97 ($N_{\text{Osc}+} = 52$; $N_{\text{Osc}-} = 45$; see Fig. 1E-F). In addition, we extracted the summed power within the 0.063~0.125 Hz range for each participant (corresponding with 8-16s, a range encompassing breathing paces used by Osc+ participants) to obtain a measure of resonance frequency oscillatory activity during biofeedback. Before conducting statistical analyses, we log transformed the power values.

Heart Rate Oscillations, Breathing Rate and End-Tidal CO₂ During fMRI Scans

The central frequency of the HF component derived from autoregressive spectral analysis was used as an alternate estimate of the breathing rate (Thayer et al., 2002). Among participants who had both breathing belt and PPG estimates of breathing, these two estimates were significantly correlated, $r(52) = 0.95, p < 0.001$, $r(56) = 0.95, p < 0.001$, $r(44) = 0.97, p < 0.001$, and $r(44) = 0.94, p < 0.001$ for the pre- and post-intervention resting-state scans and the pre- and post-intervention emotion regulation scans, respectively. Thus, for the subjects whose breathing belt respiration data were missing or not of good quality ($N = 13$ and $N = 9$ at pre- and post-intervention respectively for resting state, $N = 10$ and $N = 6$ at pre- and post-intervention respectively for emotion regulation, $N = 4$ for training-mimicking), we used the HF-HRV-derived estimate of their breathing rate. Breathing data with sudden signal drops without immediate recovery were categorized as poor quality. For these poor quality cases, breathing rate was then substituted with HF-HRV-derived estimates or excluded if the estimates were not available. We also excluded breathing data we could not precisely synchronize with fMRI data

due to failures of the scan start signal to record in the respiratory recordings. Breathing data were available for the analysis of breathing rate changes for 84 participants for resting state ($N_{Osc+} = 43$; $N_{Osc-} = 41$), 79 participants for emotion regulation ($N_{Osc+} = 45$; $N_{Osc-} = 34$), and 80 participants for training mimicking ($N_{Osc+} = 42$; $N_{Osc-} = 38$).

Exhaled carbon dioxide (CO₂) levels were measured using Philips NM3 Monitor (Model 7900) with nasal cannula. The CO₂ levels were fed to Biopac MP150 Data Acquisition System and sampled at 10kHz. After the CO₂ data were shifted with a 9-second delay and downsampled to 1kHz, peak detection was performed at the end of each breath. A time series of detected peaks were used to calculate its mean and standard deviation of end-tidal CO₂. CO₂ data were available for 73 participants ($N_{Osc+} = 38$; $N_{Osc-} = 35$) during resting state, 64 participants ($N_{Osc+} = 34$; $N_{Osc-} = 30$) during emotion regulation and 80 participants ($N_{Osc+} = 41$; $N_{Osc-} = 39$) during training mimicking. Of these, we categorized CO₂ data as poor quality if they showed sudden signal drops or stayed too low (these issues were mostly due to loosened cannulas). We excluded 27 participants ($N_{Osc+} = 13$; $N_{Osc-} = 14$) during resting state, 18 participants ($N_{Osc+} = 10$; $N_{Osc-} = 9$) during emotion regulation, 7 participants ($N_{Osc+} = 3$; $N_{Osc-} = 4$) during training mimicking. Thus, 46 participants ($N_{Osc+} = 25$; $N_{Osc-} = 21$) for resting state, 45 participants ($N_{Osc+} = 25$; $N_{Osc-} = 20$) for emotion regulation, and 73 participants ($N_{Osc+} = 38$; $N_{Osc-} = 35$) for training mimicking had CO₂ data available for the analyses.

fMRI Data

Resting State Functional Connectivity. Out of 100 participants who completed the resting state scan before and after the intervention, two participants (one person from each condition) were excluded due to unsuccessful denoising pipeline results. Additionally, two Osc+ participants were excluded because during the post-intervention resting state scan they breathed

slowly as if they were engaged in the Osc+ biofeedback. The remaining 96 participants were included in the resting-state functional connectivity analyses.

Arterial Spin Labeling. A total of 88 participants had available complete (i.e., pre- and post-intervention) pCASL data. Twenty-two participants were excluded due to errors in preprocessing or excessive motion, resulting in a total of 61 participants in subsequent pCASL analyses involving pre- and post- intervention scans, and a total of 53 participants in analyses involving pre-intervention and training scans.

Emotion Regulation Data. Ninety-eight participants ($N_{Osc+} = 52$, $N_{Osc-} = 46$) completed the emotion regulation scan before and after the intervention. Six participants ($N_{Osc+} = 3$, $N_{Osc-} = 3$) were excluded due to unsuccessful denoising pipeline results. Two participants ($N_{Osc+} = 1$, $N_{Osc-} = 1$) were excluded because task timing files were not saved correctly. Six participants ($N_{Osc+} = 3$, $N_{Osc-} = 3$) were excluded as they failed to respond to 50% or more of the trials. Eighty-four participants remained for fMRI analysis ($N_{Osc+} = 45$, $N_{Osc-} = 39$). For the emotional intensity rating analysis, we excluded an additional three subjects ($N_{Osc+} = 2$, $N_{Osc-} = 1$) whose data were collected with a malfunctioning response button device and four participants ($N_{Osc+} = 2$, $N_{Osc-} = 2$) who answered with the same number for all the trials. However, we included the six participants ($N_{Osc+} = 3$, $N_{Osc-} = 3$) for whom the fMRI denoising process was not successful. For the rating analysis, we analyzed 83 participants' responses ($N_{Osc+} = 44$, $N_{Osc-} = 39$).

Questionnaires

For the POMS, SAI, and CES-D, we fit a series of linear mixed effects models using the packages lme4 (Bates et al., 2014) and lmerTest (Kuznetsova et al., 2016) in R Version 3.6.2 (Team, 2019). For each measure, we tested fixed effects of time-point, training condition, and their interaction. For random effects, we included a random intercept for each subject, which fit

the data better for all measures than did random effects structures with intercepts at the subgroup level or for subjects nested within subgroups, as determined using likelihood ratio tests. Random effects structures including random slopes led either to unidentifiable models or singular model fits. All models were fitted using maximum likelihood. Significance of fixed effects was determined using F tests with Satterthwaite's approximation for degrees of freedom. For each measure, we performed post hoc comparisons of estimated marginal means of scores from week 1 with those from each successive week (2-7 for POMS and SAI; 2, 6 and 7 for CES-D) using the R package emmeans (Searle et al., 1980), and p-values were adjusted for multiple comparisons with a Bonferroni correction. All available data for all 106 participants were included for these analyses.

Other Measures of Heart Rate Activity

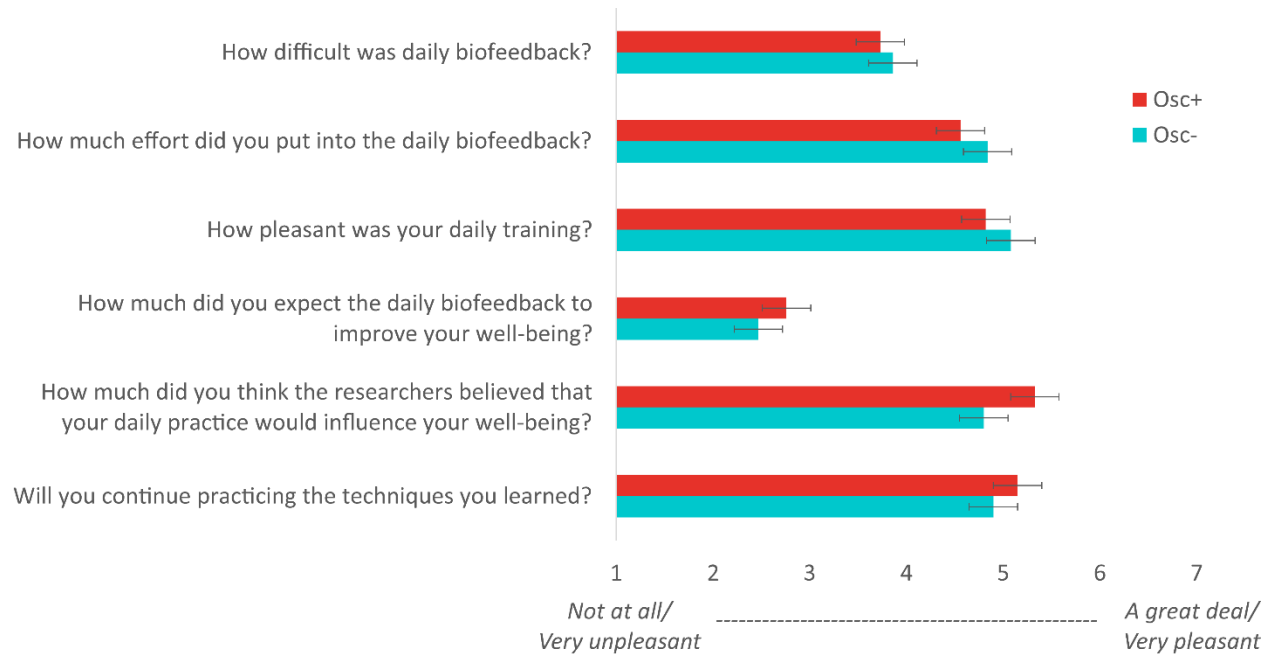
We used Kubios HRV Premium Version 3.1 to compute heart rate, the standard heart rate variability measures of low frequency HRV (LF-HRV, 0.04-0.15 Hz), high frequency HRV (HF-HRV, 0.15-0.4 Hz) and root mean squared successive difference (RMSSD) for baseline and training sessions during each lab visit. We fit separate models for heart rate, RMSSD, LF power and HF power, specifying fixed effects of time-point, training condition, and their interaction. Only data from weeks 2 and 7 were included in the statistical models to examine how each measure changed from pre- to post-training. Otherwise, we followed the same linear effect modeling set-up for these analyses as for the questionnaire data (see *Questionnaires* section above), using all available data for all 106 participants.

Supplementary Results

Post-Study Participant Perceptions of Interventions

Data for 104 participants ($N_{\text{Osc}+} = 55$; $N_{\text{Osc}-} = 49$) were included. Two participants' responses to the questionnaire were not recorded. We conducted independent t-tests to determine if there were any differences in participants' self-reported experience during the study based on their assigned condition. There were no significant differences between conditions (Supplementary Fig. 2). Specifically, there were no group differences regarding difficulty found with the biofeedback training, $t(102) = -.478, p = .633$, effort put into completing the training, $t(102) = -1.083, p = .282$, how pleasant the training was, $t(102) = -1.106, p = .271$, how much it was believed the training would impact well-being, $t(102) = .854, p = .395$, how much it was thought the researchers believed the training would impact well-being, $t(102) = 1.756, p = .082$, and plans to continue the training after the study ended, $t(102) = .840, p = .403$.

Supplementary Figure 2



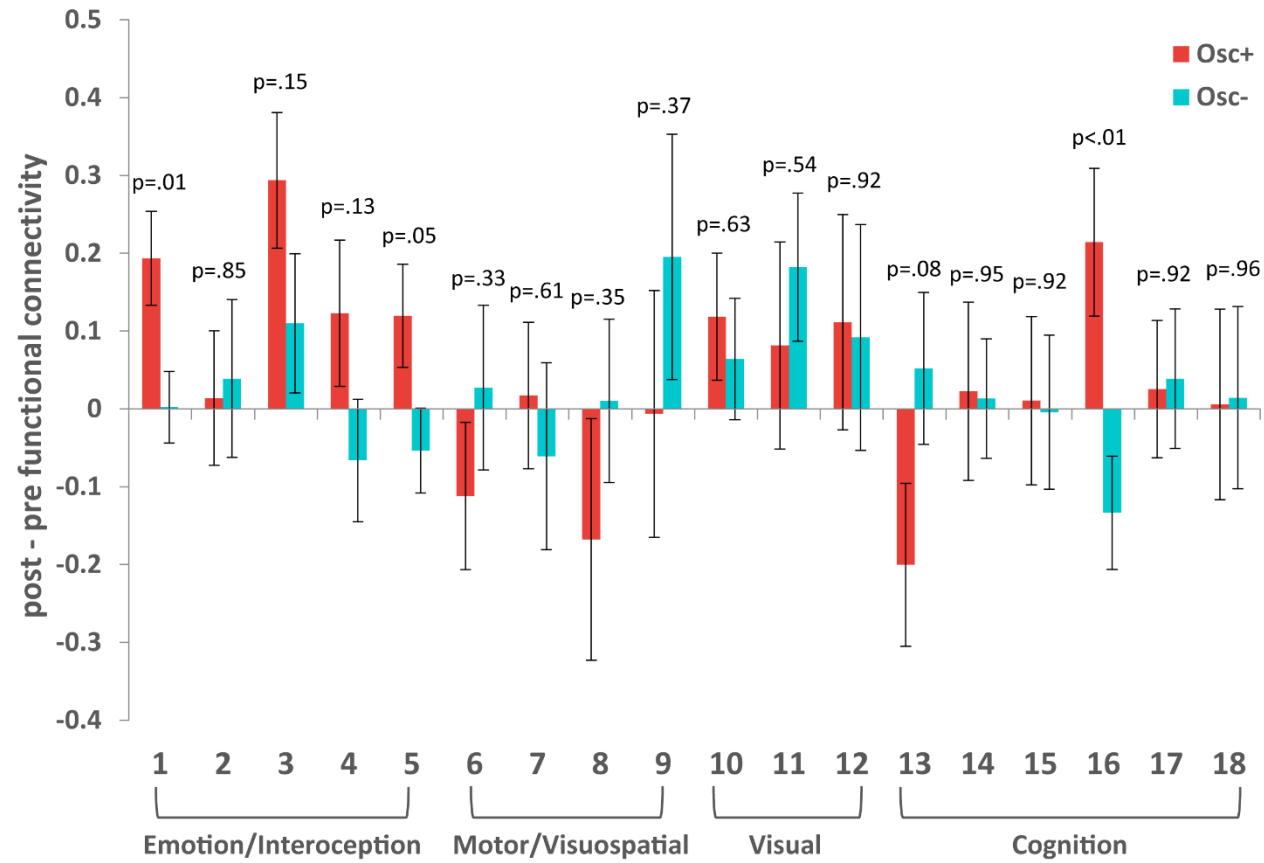
Notes. Participant average ratings in response to post-intervention questions about their expectations and effort during the study did not significantly differ between the two conditions. Error bars indicate standard errors of means.

Resting State Functional Connectivity in 18 Networks

We also examined post-pre changes in resting state functional connectivity in each of the 18 networks (Supplementary Fig. 3). Two emotion networks (Networks 1 and 5) showed significant differences between conditions ($p < .05$ FDR uncorrected), which was driven by greater post-pre changes in the Osc+ condition. Although the other three emotion/ interoception networks did not yield significant condition differences, the Osc+ participants showed a general increase in functional connectivity across the emotion/interoception category (i.e., Networks 3 and 4 also showed non-significant trends of $p < .2$ indicating relatively greater Osc+ than Osc- increases). Neither significant effects nor trends favoring the Osc+ condition were observed for any other non-emotion networks except for one cognitive network, Network 16 ($p = .005$, FDR uncorrected). This network includes the primary auditory cortices but also includes the posterior insula, which plays a key role in autonomic control. The right posterior insula has been characterized as the primary interoceptive mapping area in the cortex (Craig, 2002) and bilateral posterior insula responds to multiple modalities of interoceptive and sensory stimuli (zu Eulenburg et al., 2013). Due to the posterior insula's central role in interoception, it may be reasonable to include Network 16 in the category of emotion/interoceptive networks (which would further strengthen our results dissociating effects on emotion vs. other networks), although for our analyses we used Laird et al.'s (2011) original categorization scheme. Thus, like the analyses in the main text, these exploratory analyses of the individual networks also suggest that the Osc+ intervention strengthened functional connectivity in brain networks associated with emotion/interoception.

Supplementary Figure 3

Changes in functional connectivity



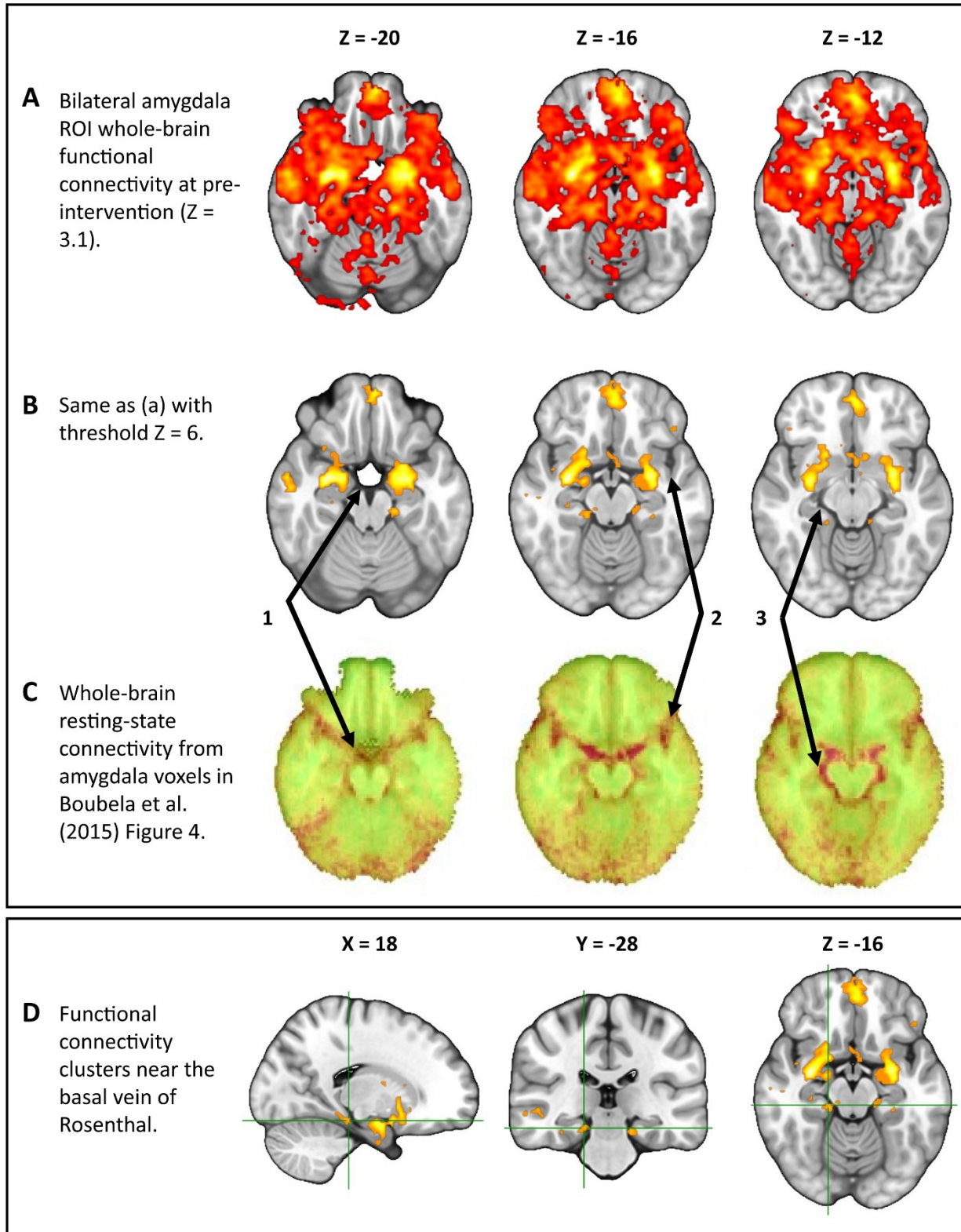
Notes. Post-intervention - pre-intervention change in functional connectivity in 18 canonical resting-state networks.

Amygdala BOLD Signal Not Driven by Signal from Basal Vein of Rosenthal

The multi-echo scanning sequence and its associated preprocessing pipeline optimizes the removal of non-BOLD signal, including non-BOLD cardiac artifacts (Kundu et al., 2017). BOLD signal from the amygdala is often contaminated by signal from the nearby basal vein of Rosenthal (Boubela et al., 2015). However, examination of whole-brain functional connectivity with bilateral amygdala ROIs in our pre-intervention data indicates that our multi-echo data collection approach and noise removal pipeline successfully avoided this confound. We used left and right amygdala as bilateral seed regions in a whole-brain functional connectivity analysis using participants' baseline pre-intervention resting-state data and examined whether the most prominent functional connectivity was with regions overlapping the basal vein of Rosenthal, as seen in many cases (Boubela et al., 2015). At the subject level, the right and left amygdala were each anatomically defined using that participant's T1 image (for more details on the segmentation and registration, see 'Resting State Functional Connectivity' in the Analyses section). We applied a low-pass temporal filter 0-0.1 Hz to the preprocessed data and extracted time series from the bilateral amygdala seed regions. For each participant, we performed a multiple regression analysis in FSL FEAT with nine regressors including the bilateral amygdala time series, signal from white matter, signal from cerebrospinal and six motion parameters. The resulting images were entered into a group analysis. Due to our large baseline N yielding high power, when thresholded at $Z = 3.1$ (Supplementary Fig. 4A), there was widespread functional connectivity making it hard to visualize where peak connectivity was. Thus, we also display the data using a higher threshold ($Z = 6$) (Supplementary Fig. 4B) to facilitate comparison with the connectivity pattern to be expected if amygdala signal mainly reflects basal vein of Rosenthal signal (Supplementary Figure 4C). As expected, the highest functional connectivity signal comes

from within the amygdala. In addition, the ventromedial PFC shows robust functional connectivity, validating the relevance of this region as a target in our functional connectivity analyses of intervention effects. Black arrows 1-3 indicate regions where signal would indicate contamination from veins. Unlike in the Boubela et al. (2015) figure, these regions are not among the voxels showing the strongest functional connectivity with the amygdala in our results. Furthermore, although there are a couple of clusters that appear to overlap the basal vein of Rosenthal (Supplementary Fig. 4D); these clusters center on the parahippocampal gyrus and follow its anatomical shape and so these clusters' connectivity signal is unlikely to be driven by signal from the vein.

Supplementary Figure 4



Notes. Whole-brain functional connectivity with bilateral amygdala at baseline during rest

thresholded at $Z = 3.1$ (A); the same results thresholded at $Z = 6$ (B); and the connectivity pattern expected if amygdala signal mainly reflects basal vein of Rosenthal signal (C). Black arrow (1) indicates that dark regions corresponding with veins are not among the regions showing the strongest functional connectivity; (2) indicates that neither are the regions around the temporal pole as shown in (C); and (3) points to the edge of the brainstem at $Z = -12$ where Boubela et al. (2015) found peak connectivity with amygdala but we did not. Row (D) provides an extended view of bilateral clusters shown in row (B) that slightly overlap with the basal vein of Rosenthal; examination of these clusters indicate that they center on the parahippocampal gyrus (see crosshairs). Panel (C) reprinted from (Boubela et al., 2015).

Emotion Regulation Task

Emotion Regulation Strategies Used and Confidence. For each emotion regulation condition, more than 95% of participants used cognitive reappraisal and more than 90% of participants indicated a medium or higher confidence level.

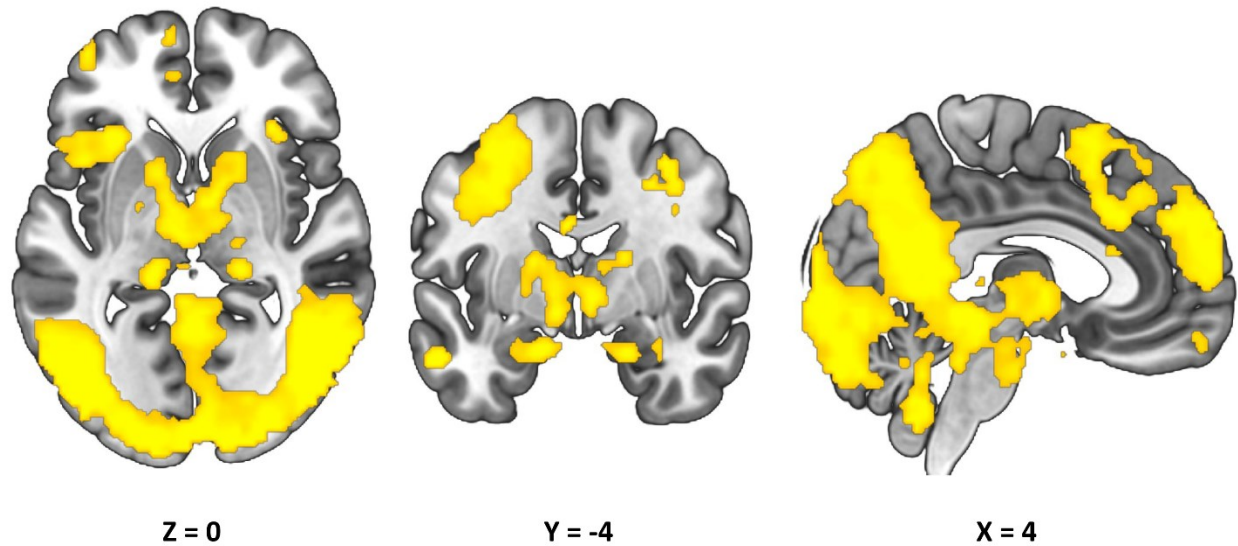
Impact of Emotional Pictures During View Condition. As a manipulation check that the emotional pictures did indeed induce more emotion-related brain activity than neutral pictures, we used whole-brain analyses to contrast brain activity during view trials that included emotional versus neutral pictures (regulation trials did not include neutral pictures). As shown in Supplementary Fig. 5, emotional pictures induced more activity in the amygdala as well as in other emotion-related brain regions such as the thalamus and anterior insula. As outlined in a separate report (Min et al., 2022), we also examined differences between diminishing and intensifying emotions at baseline and found that these two processes do not target the same set of emotion-related brain regions. When participants tried to diminish emotional reactions, they

were more likely to reduce activity in brain regions important for interoception whereas when they tried to intensify emotional reactions, they were more likely to increase activity in other emotion-related brain regions. Thus, despite a linear effect of down-regulation, control, and up-regulation (i.e., diminish < view < intensify) in subjective emotional intensity, a different set of emotion-related brain regions are targeted by the two regulatory processes. Given these marked baseline differences in how diminishing and intensifying emotions affect activity in emotion-related brain regions, in our fMRI analyses we examined the effects of down-regulation (i.e., view > diminish) and up-regulation (i.e., intensify > view) separately.

Next, we used ROI-based analyses to examine amygdala activity during emotion regulation trials. At baseline, we found significantly increased amygdala activity during intensify trials compared with view trials, $t(83) = 3.53$, $p = 0.001$, $r = 0.39$ ($M = 0.10$, $SE = 0.02$ for intensify and $M = 0.04$, $SE = 0.02$ for view) for the left amygdala and $t(83) = 1.73$, $p = 0.09$, $r = 0.19$ ($M = 0.06$, $SE = 0.02$ for intensify and $M = 0.04$, $SE = 0.02$ for view) for the right amygdala. But there were no significant differences in amygdala activity between diminish and view trials, $t(83) = 0.64$, $p = 0.53$, $r = 0.06$ ($M = 0.03$, $SE = 0.02$ for diminish and $M = 0.04$, $SE = 0.02$ for view) for the left amygdala and $t(83) = 1.18$, $p = 0.24$, $r = 0.12$ ($M = 0.02$, $SE = 0.02$ for diminish and $M = 0.04$, $SE = 0.02$ for view) for the right amygdala.

Supplementary Figure 5

Brain regions significantly activated during viewing emotional vs. neutral images at pre-intervention

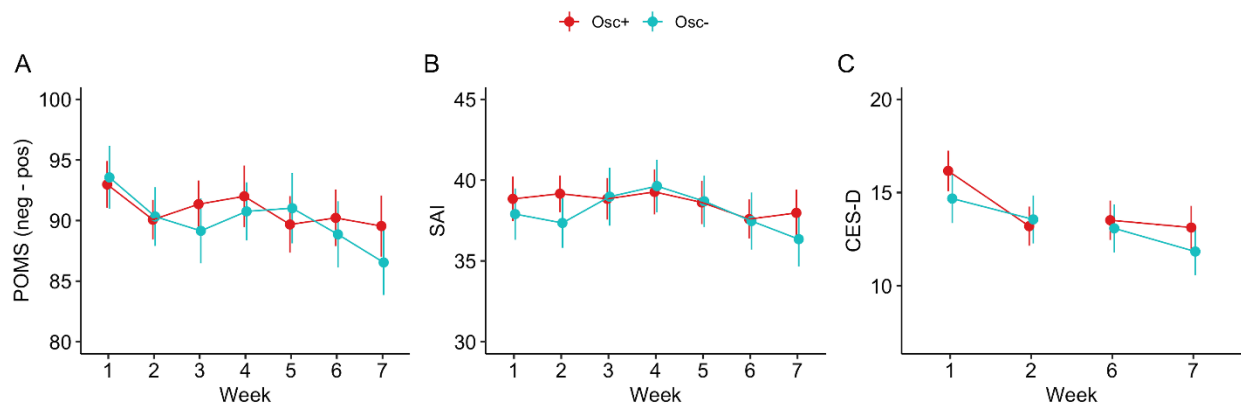


Questionnaires

See Supplementary Fig. 6 for mean POMS, SAI, and CES-D scores across the duration of the study. Using linear mixed effects models, we found a significant main effect of time-point on POMS scores, $F(6,625.40) = 2.47$, $p = .023$, $r = .14$, but no significant main effect of training condition, $F(1,106.08) = 0.05$, $p = .830$, $r = .02$, or time-point by training condition interaction effect, $F(6,625.40) = 0.70$, $p = .653$, $r = .08$. Post hoc comparisons indicated that POMS scores were significantly lower at week 7 compared to week 1, $t(637.46) = -3.56$, $p = .002$, $r = -0.14$. No other post hoc comparisons yielded significant results (all p 's $> .05$). A similar approach indicated no significant effects of time-point, $F(6,622.17) = 1.80$, $p = .097$, $r = .14$, training condition, $F(1,105.83) = 0.06$, $p = .809$, $r = .02$, or their interaction, $F(6,622.17) = 0.961$, $p = .451$, $r = .09$, on SAI scores. Finally, we found a significant main effect of time-point on CES-D

scores, $F(3, 313.99) = 6.48, p < .001, r = .24$, but no significant effect of training condition, $F(1,105.72) = 0.14, p = .709, r = .03$, or interaction effect between time-point and training condition, $F(3,313.99) = 0.93, p = .425, r = .09$. Post hoc comparisons indicated that, compared to Week 1, CES-D scores were significantly lower at Week 2, $t(320.38) = -2.85, p = .014, r = -0.16$, Week 6, $t(320.38) = -2.85, p = .014, r = -0.16$, and Week 7, $t(320.38) = -4.24, p < .001, r = -0.23$.

Supplementary Figure 6



Notes. Mean scores on the Profile of Mood States (POMS; A), State Anxiety Inventory (SAI; B), and Center for Epidemiological Studies Depression Scale (CES-D; C) during weekly lab visits for participants in the Osc+ (red) and Osc- (blue) conditions. Higher POMS scores reflect greater negative affect, higher SAI scores reflect greater state anxiety, and higher CES-D scores reflect a higher depression quotient. A constant value of 100 was added to POMS scores to eliminate negative values. The CES-D was not administered in weeks 3, 4 or 5. Error bars reflect standard errors of the mean.

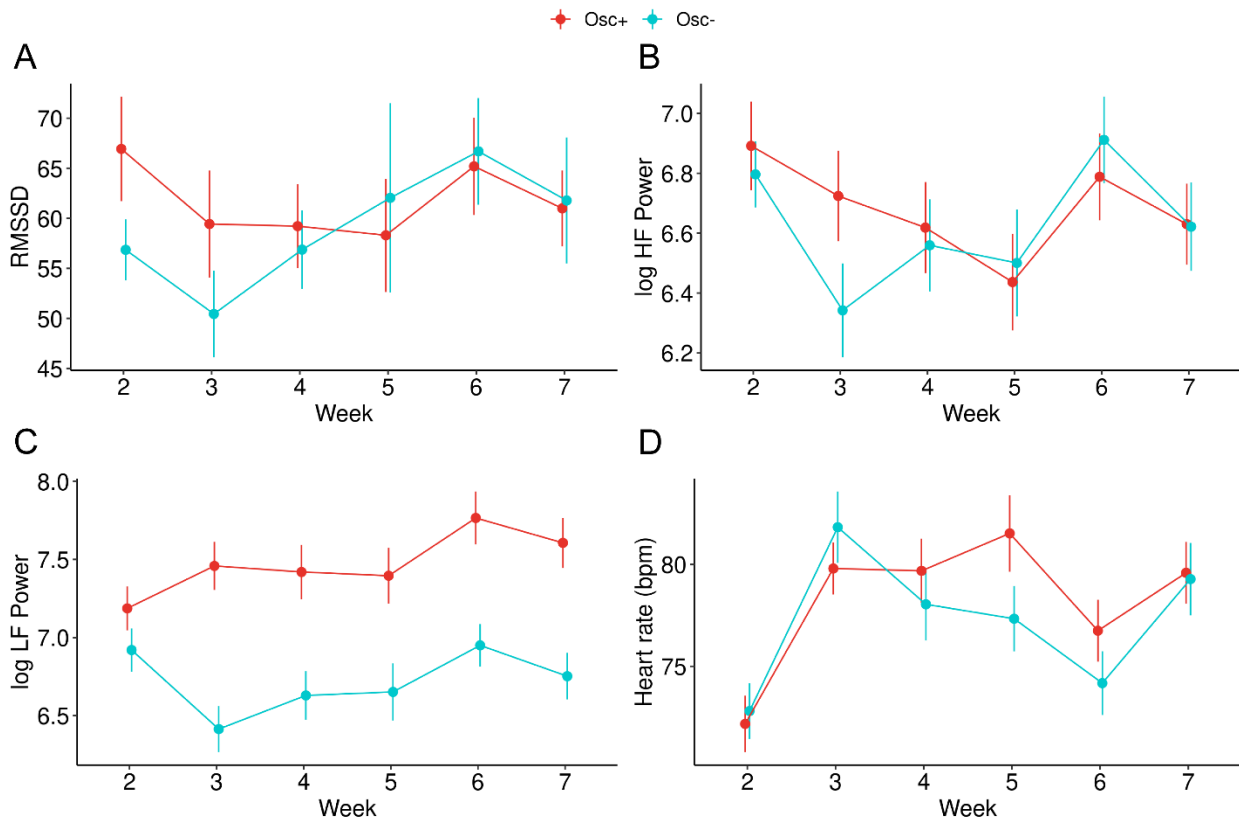
Heart Rate Variability and Heart Rate During Seated Rest Across Study

RMSSD, HF power, LF power and mean heart rate at seated rest across the course of the study are displayed in Supplementary Fig. 7. Using linear mixed effects models, we did not find significant main effects of time-point (pre- vs. post-intervention or Week 2 vs. Week 7), $F(1,102) = 0.02, p = .898, r = .01$, or training condition, $F(1,102) = 0.74, p = .391, r = .09$, nor a significant interaction effect between time-point and training condition on RMSSD, $F(1,102) = 1.91, p = .170, r = .14$. In contrast, this approach indicated a significant main effect of time-point on HF power, $F(1,102) = 4.04, p = .047, r = .20$, but no significant main effect of training condition, $F(1,102) = 0.10, p = .748, r = .03$, or interaction effect between time-point and training condition, $F(1,102) = 0.16, p = .689, r = .04$. In addition, we found a significant main effect of training condition, $F(1,102) = 11.62, p < .001, r = .32$, as well as a significant interaction effect between training condition and time-point, $F(1, 102) = 5.11, p = .026, r = .22$, on LF power. We did not observe a significant main effect of time-point on LF power, $F(1,102) = 0.94, p = .334, r = .10$. Post-hoc comparisons indicated significant increases in LF power from pre- to post-intervention in the Osc+ group, $t(104) = 2.38, p = .019, r = .11$, and non-significant decreases in LF power in the Osc- group, $t(104) = -0.86, p = .391, r = .04$. Finally, we found a significant main effect of time-point on heart rate, $F(1,102) = 42.41, p < .001, r = .54^1$, but no main effect of training condition, $F(1,102) = 0.01, p = .930, r = .01$, or interaction effect between time-point and training condition, $F(1,102) = 0.19, p = .660, r = .04$. This pattern of results did

¹ The increased heart rate at week 7 may be due to differences in measurement timing between Weeks 2 and 7. On Week 2, heart rate was measured approximately 30 minutes after the MRI scan since we did not want to introduce the biofeedback training, which starts with a baseline measure of heart rate, until after the scan which assessed the pre-intervention state. On week 7, most participants' heart rate was measured within 30 minutes after their arrival to the lab (before the scan), as we did on Weeks 3-6. Heart rate was particularly low on Week 2 due perhaps to the fact that they had just been lying down in the scanner for an hour. Participants in the two conditions experienced the same protocol for order of tasks.

not change when excluding participants identified as outliers based on total spectral power (see *Heart Rate Oscillations During Training* in Methods).

Supplementary Figure 7



Notes. Mean resting root mean squared successive differences (RMSSD; A), high-frequency (HF) power (B), low-frequency (LF) power (C), and heart rate (D) during weekly lab visits for participants in the Osc+ (red) and Osc- (blue) conditions. Error bars reflect standard errors of the mean.

Effects of Health Status on Outcomes

Although our participants were relatively healthy young adults, some reported that they had previously been diagnosed with major illnesses and/or currently taking medication (Supplementary Table 3). Thus, we performed analyses including health status as a covariate. We coded health status as “1” if the participant reported that they had been diagnosed with major illnesses (e.g., asthma, osteoporosis, seizures) and/or currently taking medication. We coded “0” otherwise. As detailed below, the patterns of results remained the same with the covariate.

Resting-state Functional Connectivity in Emotion Networks. The condition (Osc+, Osc-) by network category (emotion/interoception, other) interaction remained significant, $F(1, 93) = 5.36, p = .023, r = .23$.

Resting-state Functional Connectivity Between MPFC and Amygdala. The condition by time-point interaction for mPFC-right amygdala connectivity remained non-significant, $F(1, 93) = 0.62, p = .43, r = .08$. The interaction for mPFC-left amygdala connectivity remained significant at uncorrected $p < .05, F(1, 93) = 4.79, p = .031, r = .22$ (although it did not quite meet the Benjamini-Hochberg corrected significance level of .025).

Emotion Regulation (Amygdala ROI Analyses). Pre-to-post change in left amygdala activity did not differ between conditions, $F(1, 81) = .000, p = .996, r = .00$ for Intensify > View, and $F(1, 81) = 1.88, p = .17, r = .15$ for View > Diminish. Also, pre-to-post change in right amygdala activity did not differ between conditions, $F(1, 81) = .77, p = .38, r = .10$ for Intensify > View, and $F(1, 81) = .23, p = .63, r = .06$ for View > Diminish.

Emotion Regulation (Whole-brain Analyses). The clusters remained the same for all contrasts (Fig. 5 and Supplementary Table 5) after including the health status covariate.

Emotion Regulation (Rating). There were no significant multiple-comparison-corrected effects of condition or time-point on ratings during Diminish, View and Intensify trials.

Supplementary Table 1

Age, sex, education, and baseline mood, anxiety and depression ratings across intervention conditions

	OSC+ (N = 56)		OSC- (N = 50)		Group difference
	Mean (SD)	Min-Max	Mean (SD)	Min-Max	<i>p</i> value
Age	22.80 (2.42)	18-28	22.60 (3.17)	18-31	.71
Gender	1.48 (0.50)	N/A	1.52 (0.51)	N/A	.70
Years Education	16.08 (1.75)	12-20	15.74 (2.58)	12-24	.42
POMS Baseline	92.80 (14.23)	68-139	93.56 (18.31)	68-166	.81
SAI Baseline	38.84 (10.30)	21-65	37.90 (11.24)	20-68	.65
TAI Baseline	42.73 (10.03)	22-67	41.38 (12.46)	21-70	.54
CESD Baseline	15.96 (8.11)	4-37	14.68 (9.31)	2-45	.45

Notes. Osc+=increase-oscillations; Osc-=decrease-oscillations; POMS=Profile of Mood States (Grove & Prapavessis, 1992); SAI=State Anxiety Inventory (Spielberger & Gorsuch, 1983); TAI=Trait Anxiety Inventory (Spielberger & Gorsuch, 1983); CESD=Center for Epidemiological Studies Depression Scale (Radloff, 1977)

Supplementary Table 2

Race of participants across intervention conditions

Race	OSC+ (N = 56)	OSC- (N = 50)
African American	4	0
Asian	41	34
Bi-racial	1	1
Caucasian	7	12
Other	2	3
Prefer not to state	1	0

Notes. Among these, 2 Osc+ and 4 Osc- participants identified as being of Hispanic ethnicity.

Supplementary Table 3

Number of participants who had been diagnosed with major illnesses and who were on medication at the time of their study participation

	Osc+ (N = 56)	Osc- (N = 50)	Difference between conditions
Medical condition (Total N)	2	5	$p = 0.10$
Asthma	1	0	
High cholesterol	0	1	
Osteoporosis or tendonitis	0	2	
Seizures	1	1	
Ulcers	0	1	
Medication (Total N)	9	11	$p = 0.44$
Birth control pill	6	6	
Pain medication	2	1	
Psychiatric medication	0	3	
Sedative/hypnotic	1	0	
Vitamin/herbal supplement	0	1	

Supplementary Table 4

Activity levels within the amygdala region-of-interest (percent signal change) during the emotion regulation task

ROI	OSC+				OSC-			
	Pre		Post		Pre		Post	
	M	SE	M	SE	M	SE	M	SE
Left amygdala								
Diminish	0.03	0.02	0.03	0.02	0.02	0.02	0.02	0.02
View	0.03	0.02	0.02	0.02	0.05	0.03	0.02	0.02
Intensify	0.11	0.03	0.12	0.03	0.10	0.03	0.07	0.03
Right amygdala								
Diminish	0.02	0.02	0.08	0.03	0.02	0.02	0.02	0.02
View	0.03	0.02	0.07	0.02	0.04	0.02	0.00	0.03
Intensify	0.05	0.02	0.11	0.03	0.07	0.02	0.07	0.03

Supplementary Table 5

Whole-brain significant clusters and locations of local maxima during emotion regulation scan

(A) time by condition interaction for View > Diminish (B) OSC+ Post > Pre for View >

Diminish (C) OSC- Post > Pre for View > Diminish, with regions located based on Harvard-

Oxford cortical and subcortical structural atlases

(A) Time by condition interaction for View > Diminish

Cluster	Voxels	<i>p</i>	<i>Z</i>	MNI (x, y, z)			Regions of local maxima
4	1305	0.0386	3.54	14	-40	64	Postcentral gyrus
			3.54	18	-42	56	White matter adjacent to postcentral gyrus
			3.54	40	-44	56	Superior parietal lobule
			3.54	22	-24	54	White matter adjacent to precentral gyrus
			3.54	42	-40	54	Superior parietal lobule, posterior supramarginal gyrus
			3.54	14	-42	54	Precuneus cortex, postcentral gyrus
3	126	0.0444	3.54	-2	-46	42	Precuneus cortex, posterior cingulate gyrus
			3.54	-2	-52	58	Precuneus cortex
			3.54	-8	-54	64	Precuneus cortex, superior parietal lobule
			3.35	-8	-54	60	Precuneus cortex
			3.24	-2	-48	52	Precuneus cortex
			3.24	-8	-54	56	Precuneus cortex
2	65	0.042	3.54	34	-2	-2	White matter overlapping putamen
			3.54	40	-2	0	Insula

1	37	0.0378	3.54	-18	-60	56	Superior lateral occipital cortex, superior parietal lobule
---	----	--------	------	-----	-----	----	--

(B) OSC+ Post > Pre for View > Diminish

Cluster	Voxels	<i>p</i>	<i>Z</i>	MNI (x, y, z)			Regions of local maxima
4	7245	0.0026	3.54	18	-42	60	Postcentral gyrus
			3.24	18	-20	60	White matter adjacent to precentral gyrus
			3.09	34	-6	-14	White matter adjacent to amygdala
			3.09	24	-22	68	Precentral gyrus
			3.09	0	2	40	Anterior cingulate gyrus
			3.09	-18	-56	58	Superior parietal lobule
3	78	0.0424	2.33	40	-40	56	Superior parietal lobule
			2.23	38	-34	56	Postcentral gyrus
2	60	0.0366	3.04	46	28	-4	Frontal orbital cortex
1	49	0.0386	3.04	64	-14	16	Postcentral gyrus, central opercular cortex
			2.71	58	-14	12	Central opercular cortex

(C) OSC- Post > Pre for View > Diminish

Cluster	Voxels	<i>p</i>	<i>Z</i>	MNI (x, y, z)			Regions of local maxima
2	50	0.0238	3.54	-8	100	6	Occipital pole
			3.54	-8	-96	14	Occipital pole
1	22	0.0352	3.24	16	-94	16	Occipital pole

Supplementary Table 6*Ratings of feeling strength during each condition of the emotion regulation task*

Conditio ns	OSC+				OSC-			
	Pre		Post		Pre		Post	
	Mean	Std. Error						
Diminish negative	1.86	0.08	1.91	0.07	1.88	0.09	2.01	0.09
View negative	2.12	0.09	1.95	0.08	2.40	0.10	2.42	0.11
Intensify negative	3.15	0.08	3.35	0.08	3.26	0.09	3.41	0.07
Diminish positive	1.82	0.10	1.81	0.08	1.76	0.09	1.91	0.09
View positive	2.03	0.09	1.97	0.08	2.21	0.10	2.43	0.10
Intensify positive	3.14	0.09	3.19	0.09	3.29	0.09	3.38	0.07
View neutral	1.34	0.07	1.31	0.07	1.32	0.08	1.48	0.10

Supplementary Table 7

Comparison of physiology metrics across the two conditions during pre- and post-intervention resting-state and emotion-regulation scans

Measure	OSC-		OSC+		Statistical Comparison*
	Pre	Post	Pre	Post	
Physiology during resting-state fMRI scan					
Breathing frequency (Hz)	.29 (.01)	.29 (.01)	.28 (.01)	.27 (.01)	$F(1, 82) = 2.15, p = .15, r = .16$
End-tidal CO2 (mmHg)	40.24 (.90)	40.18 (.91)	40.60 (.83)	40.65 (.83)	$F(1, 44) = .007, p = .94, r < .001$
Standard deviation of end-tidal CO2 (mmHg)	1.37 (.16)	1.16 (.11)	1.47 (.15)	1.49 (.10)	$F(1, 44) = 0.76, p = .39, r = .13$
Heart rate (bpm)	70.06 (1.47)	68.55 (1.43)	69.39 (1.45)	67.18 (1.41)	$F(1,77) = .13, p = .725, r = .04$
RMSSD (ms)	45.14 (4.73)	49.57 (6.89)	53.47 (4.67)	62.12 (6.81)	$F(1,77) = .48, p = .49, r = .08$
LF-HRV (log of ms ²)	6.45 (.13)	6.59 (.13)	6.41 (.13)	6.87 (.17)	$F(1,77) = 2.0, p = .16, r = .16$
HF-HRV (log of ms ²)	6.51 (.16)	6.59 (.17)	6.62 (.16)	6.87 (.17)	$F(1,77) = .84, p = .36, r = .10$
Physiology during emotion regulation fMRI scan					
Breathing frequency (Hz)	.29 (.01)	.29 (.01)	.27 (.01)	.26 (.01)	$F(1, 77) = 1.31, p = .26, r = .13$
End-tidal CO2 (mmHg)	39.13 (.90)	39.71 (.85)	40.25 (.84)	39.92 (.80)	$F(1, 43) = .54, p = .47, r = .11$
Standard deviation of end-tidal CO2 (mmHg)	1.04 (.11)	1.00 (.09)	1.39 (.10)	1.27 (.09)	$F(1, 43) = .32, p = .58, r = .08$

Heart rate (bpm)	72.79 (1.53)	68.42 (1.31)	67.94 (1.49)	66.13 (1.27)	$F(1, 70) = 1.57, p = .22, r = .15$
RMSSD (ms)	41.77 (5.06)	53.88 (6.79)	61.06 (4.92)	64.75 (6.61)	$F(1, 70) = 1.68, p = .20, r = .15$
LF-HRV (log of ms ²)	6.44 (.14)	6.85 (.13)	6.65 (.14)	6.95 (.13)	$F(1, 70) = .44, p = .51, r = .08$
HF-HRV (log of ms ²)	6.41 (.17)	6.74 (.17)	6.91 (.16)	6.93 (.17)	$F(1, 70) = 2.09, p = .15, r = .17$

Notes. Statistical tests are 2 (time-point: pre, post) X 2 (condition: Osc+, Osc-) ANOVAs for scan sessions with both pre and post data. Standard errors in parentheses.

Supplementary Table 8

Comparison of physiology metrics across the two conditions during the training-mimicking fMRI scan

	OSC-	OSC+	Statistical Comparison*
	Post	Post	
Breathing frequency (Hz)	.26 (.01)	.10 (.003)	$t(78) = -17.36, p < .001, r = .89$
End-tidal CO2 (mmHg)	40.74 (.79)	39.92 (.74)	$t(71) = -.76, p = .45, r = .09$
Standard deviation of end-tidal CO2 (mmHg)	1.32 (.11)	1.75 (.12)	$t(71) = 2.67, p = .01, r = .30$
Heart rate (bpm)	66.67 (1.35)	65.52 (1.24)	$t(76) = .63, p = .27, r = .07$
RMSSD (ms)	59.11 (6.34)	63.88 (5.98)	$t(76) = -.55, p = .29, r = .06$
LF-HRV (log of ms ²)	6.93 (.13)	8.56 (.11)	$t(76) = -9.54, p < .001, r = .73$

Supplementary References

- Bates, D., Mächler, M., Bolker, B., & Walker, S. (2014). Fitting linear mixed-effects models using lme4. *Journal of Statistical Software*, 67(1). <https://doi.org/10.18637/jss.v067.i01>
- Bennett, D. H., Holmes, D. S., & Frost, R. O. (1978). Effects of instructions, biofeedback, reward, and cognitive mediation on the control of heart rate and the application of that control in a stressful situation. *Journal of Research in Personality*, 12(4), 416-430.
- Boubela, R. N., Kalcher, K., Huf, W., Seidel, E.-M., Derntl, B., Pezawas, L., Našel, C., & Moser, E. (2015). fMRI measurements of amygdala activation are confounded by stimulus correlated signal fluctuation in nearby veins draining distant brain regions. *Scientific Reports*, 5(1), 10499. <https://doi.org/10.1038/srep10499>
- Craig, A. D. (2002). How do you feel? Interoception: the sense of the physiological condition of the body. *Nature Reviews Neuroscience*, 3(8), 655-666.
- Faul, F., Erdfelder, E., Lang, A. G., & Buchner, A. (2007). G*Power 3: A flexible statistical power analysis program for the social, behavioral, and biomedical sciences. *Behavior Research Methods*, 39(2), 175-191. <Go to ISI>://000248501300003
- Grove, J. R., & Prapavessis, H. (1992). Preliminary evidence for the reliability and validity of an abbreviated profile of mood states. *International Journal of Sport Psychology*.
- Kundu, P., Voon, V., Balchandani, P., Lombardo, M. V., Poser, B. A., & Bandettini, P. A. (2017). Multi-echo fMRI: A review of applications in fMRI denoising and analysis of BOLD signals. *Neuroimage*, 154, 59-80. <https://doi.org/https://doi.org/10.1016/j.neuroimage.2017.03.033>
- Kuznetsova, A., Brockhoff, P., & Christensen, R. (2016). Tests in linear mixed effects models version. *Cran*. URL <https://cran.r-project.org/web/packages/lmerTest/lmerTest.pdf>.
- Laird, A. R., Fox, P. M., Eickhoff, S. B., Turner, J. A., Ray, K. L., McKay, D. R., Glahn, D. C., Beckmann, C. F., Smith, S. M., & Fox, P. T. (2011). Behavioral interpretations of intrinsic connectivity networks. *Journal of Cognitive Neuroscience*, 23(12), 4022-4037.
- Lang, P. J., Bradley, M. M., & Cuthbert, B. N. (1999). *The international affective picture system (IAPS): Technical manual and affective ratings*.
- Lehrer, P., Vaschillo, B., Zucker, T., Graves, J., Katsamanis, M., Aviles, M., & Wamboldt, F. (2013). Protocol for heart rate variability biofeedback training. *Biofeedback*, 41(3), 98-109.
- Min, J., Nashiro, K., Yoo, H. J., Cho, C., Nasser, P., Bachman, S. L., Porat, S., Thayer, J. F., Chang, C., & Lee, T.-H. (2022). Emotion Downregulation Targets Interoceptive Brain Regions While Emotion Upregulation Targets Other Affective Brain Regions. *Journal of Neuroscience*, 42(14), 2973-2985.
- Radloff, L. S. (1977). The CES-D Scale: A self-report depression scale for research in the general population. *Applied Psychological Measurement*, 1, 385-401.
- Sarmiento, S., García-Manso, J. M., Martín-González, J. M., Vaamonde, D., Calderón, J., & Da Silva-Grigoletto, M. E. (2013). Heart rate variability during high-intensity exercise. *Journal of Systems Science and Complexity*, 26(1), 104-116.
- Searle, S. R., Speed, F. M., & Milliken, G. A. (1980). Population marginal means in the linear model: an alternative to least squares means. *The American Statistician*, 34(4), 216-221.
- Spielberger, C. D., & Gorsuch, R. L. (1983). *Manual for the State-Trait Anxiety Inventory (Form Y) ("Self-Evaluation Questionnaire")* Consulting Psychologists Press.

- Tarvainen, M. P., Niskanen, J.-P., Lipponen, J. A., Ranta-Aho, P. O., & Karjalainen, P. A. (2014). Kubios HRV—heart rate variability analysis software. *Computer Methods and Programs in Biomedicine*, *113*(1), 210-220.
- Team, R. C. (2019). *R: A language and environment for statistical computing*. R Foundation for Statistical Computing. In
- Thayer, J. F., Sollers, J. J., Ruiz-Padial, E., & Vila, J. (2002). Estimating respiratory frequency from autoregressive spectral analysis of heart period. *IEEE Engineering in Medicine and Biology Magazine*, *21*(4), 41-45.
- zu Eulenburg, P., Baumgärtner, U., Treede, R. D., & Dieterich, M. (2013). Interoceptive and multimodal functions of the operculo-insular cortex: Tactile, nociceptive and vestibular representations. *Neuroimage*, *83*, 75-86.
<https://doi.org/https://doi.org/10.1016/j.neuroimage.2013.06.057>